ISSCR

miRNome Profiling of Purified Endoderm and Mesoderm Differentiated from hESCs Reveals Functions of miR-483-3p and miR-1263 for Cell-Fate Decisions

Daichi Ishikawa,[1,2,5] Ulf Diekmann,[1,5] Jan Fiedler,[3] Annette Just,[3] Thomas Thum,[3,4] Sigurd Lenzen,[1] and Ortwin Naujok[1,*]

[1]Institute of Clinical Biochemistry, Hannover Medical School, Carl-Neuberg-Straße 1, 30625 Hannover, Germany
[2]Department of Surgery, Tokushima University, 3-18-15, Kuramoto, Tokushima 770-8503, Japan
[3]Institute of Molecular and Translational Therapeutic Strategies (IMTTS), Hannover Medical School, Carl-Neuberg-Straße 1, 30625 Hannover, Germany
[4]National Heart and Lung Institute, Imperial College London, Sydney Street, London SW3 6NP, UK
[5]Co-first author
*Correspondence: naujok.ortwin@mh-hannover.de
 https://doi.org/10.1016/j.stemcr.2017.10.011

SUMMARY

Pluripotent stem cells hold great promise for regenerative medicine since they can differentiate into all somatic cells. MicroRNAs (miRNAs) could be important for the regulation of these cell-fate decisions. Profiling of miRNAs revealed 19 differentially expressed miRNAs in the endoderm and 29 in the mesoderm when analyzing FACS-purified cells derived from human embryonic stem cells. The mesodermal-enriched miR-483-3p was identified as an important regulator for the generation of mesodermal PDGFRA$^+$ paraxial cells. Repression of its target PGAM1 significantly increased the number of PDGFRA$^+$ cells. Furthermore, miR-483-3p, miR-199a-3p, and miR-214-3p might also have functions for the mesodermal progenitors. The endoderm-specific miR-489-3p and miR-1263 accelerated and increased endoderm differentiation upon overexpression. KLF4 was identified as a target of miR-1263. RNAi-mediated downregulation of KLF4 partially mimicked miR-1263 overexpression. Thus, the effects of this miRNA were mediated by facilitating differentiation through destabilization of pluripotency along with other not yet defined targets.

INTRODUCTION

During vertebrate development one of the first cell-fate decisions is gastrulation, resulting in the formation of three embryonic germ layers (Murry and Keller, 2008). During gastrulation the definitive endoderm (DE) and mesoderm (ME) arise, with evidence that they originate from a mesendodermal progenitor (Murry and Keller, 2008; Yang et al., 2014). Human pluripotent stem cells (hPSCs) such as embryonic stem cells (hESCs) or induced pluripotent stem cells (hiPSCs) can differentiate under appropriate conditions into virtually any adult cell type. These cells can be used to study human development *in vitro* or provide a cell source for regenerative medicine. However, despite extensive studies of transcriptional networks and dynamics in model organisms and during hPSC differentiation, many aspects of gene regulation during germ layer formation are not well understood.

Endogenous non-coding RNAs, such as microRNAs (miRNAs), are regulatory elements that can control the expression of target genes on the post-transcriptional level (Bartel, 2009). They exert important functions in development, differentiation, cell-fate specification, and pathogenesis (Eliasson and Esguerra, 2014; Fiedler et al., 2014; Sayed and Abdellatif, 2011). Knockout of the miRNA-processing proteins Dicer1 or Dgcr8 results in lethality during embryogenesis and disturbed ESC differentiation, demonstrating that miRNAs possess essential functions for early development (Bernstein et al., 2003; Wang et al., 2007;

Kanellopoulou et al., 2005). Additionally, miRNAs can facilitate reprogramming of somatic cells into iPSCs and help to maintain pluripotency (Leonardo et al., 2012). Several studies identified miRNA clusters that are highly enriched in PSCs with decreasing expression levels upon differentiation, such as the species-conserved miR-302/367 or the human miR-371–373 cluster (ortholog of the murine miR-290–295 cluster) (Chen et al., 2007; Diekmann et al., 2013; Lakshmipathy et al., 2010; Laurent et al., 2008; Stadler et al., 2010). However, miRNAs enriched in ESCs can exhibit additional functions during early differentiation, as shown across different species for the miR-430/427/302 family that is also important for proper endoderm and mesoderm development (Rosa et al., 2009).

Studies of the miRNA transcriptome (miRNome) during DE differentiation of hESCs revealed a unique miRNA expression profile (Fogel et al., 2015; Hinton et al., 2010, 2014; Liao et al., 2013) but these studies analyzed heterogeneous cultures, which did not allow a reliable correlation between miRNA expression and the DE. Therefore, this study comparatively analyzed the miRNome of hESCs from fluorescence-activated cell sorting (FACS)-purified DE and ME to identify differentially expressed miRNAs. Identified miRNAs were functionally analyzed during differentiation, *in silico* predicted target mRNAs were analyzed by a luciferase reporter assay, and effects of these genes upon differentiation were investigated. Out of the DE candidate miRNAs miR-489-3p, miR-1263, and the miR-371–373 cluster were primarily expressed in DE cells.
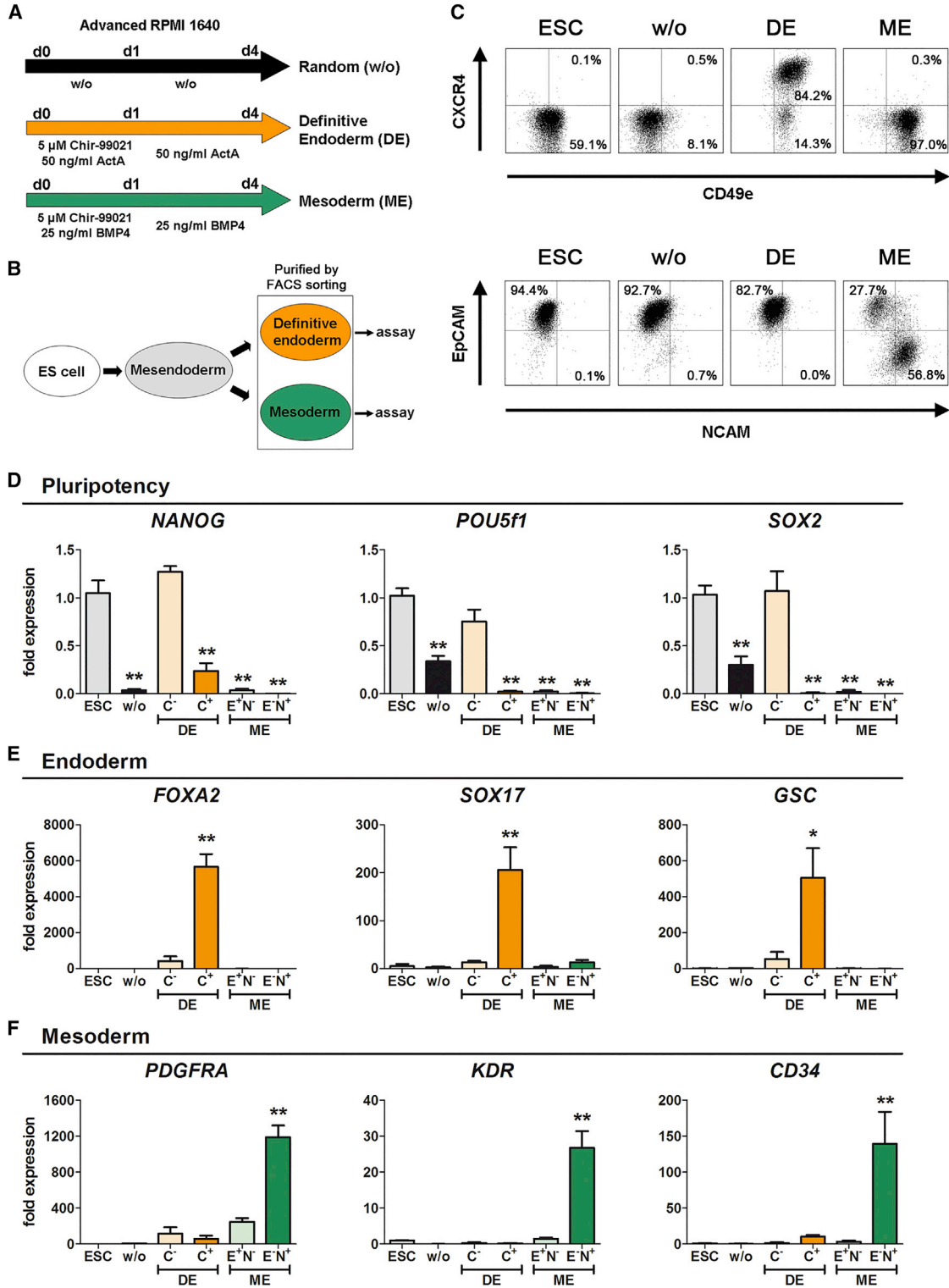
CrossMark

Figure 1. Characterization of Sorted Cell Populations

(A) Protocols used for randomized, endoderm (DE), and mesoderm (ME) differentiation.

(B) Schematic overview of the experimental setup to purify the different populations.

(legend continued on next page)

Transfection with miR-1263 and/or miR-489-3p mimics increased the number of CXCR4$^+$ DE cells and accelerated DE differentiation. The pluripotency regulator KLF4 was regulated by miR-1263 on the mRNA and protein expression level. Additionally, repression of KLF4 by small interfering RNA (siRNA) partially mimicked this effect. The miRNAs miR-199a-3p, miR-214-3p, and miR-483-3p were highly enriched in ME cells. Functional analysis revealed that only miR-483-3p was able to alter the composition of the analyzed ME subpopulations. PGAM1 was identified as an mRNA target of miR-483-3p, which was also regulated on the protein level. The miR-483-3p effect was in part mimicked by PGAM1 repression. Thus, this study showed that miR-1263 facilitates DE differentiation likely by KLF4 repression, while miR-483-3p has an important function for subdividing the broad ME into progenitor subpopulations for further lineage specification.

RESULTS

Characterization of Sorted Populations upon Differentiation

Initially, several protocols were tested to induce ME from hESCs, with highest expression values of mesodermal genes (*KDR*, *PDGFRA*, *MEOX1*, *CD34*) using protocol ME3 (Figures S1A and S1B). In line with the role of *T* (Bry) for early mesendo/mesoderm specification (Tan et al., 2013), ME3 induced its peak expression early if GSK3 inhibition by CHIR-99021 (CHIR), to activate Wnt/β-catenin signaling, was present, and a decreased expression thereafter (Figure S1C). GSK3 inhibition for more than 2 days (ME1, ME5) or together with fibroblast growth factor 2 supplementation (ME4) reduced the expression of *KDR* and *PDGFRA* (Figure S1B). A nearly identical expression profile was obtained with the second hESC line, HUES8 (Figure S1D). Thus, ME3 was used for the mesoderm differentiation in the following experiments.

Figure 1A shows the applied differentiation protocols to purify endoderm and ME by FACS (Figure 1B). CXCR4 was solely induced upon differentiation toward the DE, while CD49e, a described marker for DE progeny (Wang et al., 2011), was additionally detected upon ME differentiation (Figure 1C). EpCAM was highly expressed on hESCs and maintained under DE or randomized conditions.

Upon ME differentiation EpCAM decreased while NCAM$^+$ cells appeared (Figure 1C). Time-course analysis during ME differentiation revealed early EpCAM/NCAM double-positive cells at day 2, which decreased their EpCAM positivity upon further differentiation (Figure S1E). Hence, EpCAM$^-$/NCAM$^+$ and EpCAM$^+$/NCAM$^-$ cells after ME differentiation as well as CXCR4$^+$ and CXCR4$^-$ cells upon DE differentiation were characterized in detail.

The CXCR4$^-$ population exhibited similar expression levels of *NANOG*, *POU5f1*, and *SOX2* compared with hESCs, suggesting that these cells resisted endodermal differentiation and maintained pluripotency (Figure 1D). In contrast, CXCR4$^+$ cells and both populations upon ME differentiation showed very low expression levels of these pluripotency marker genes (Figure 1D). The DE marker genes *SOX17*, *FOXA2*, *GSC*, and *MIXL1* were highly expressed only in CXCR4$^+$ cells (Figures 1E and S2A), while the ME marker genes *PDGFRA*, *KDR*, *CD34*, *MEOX1*, and *OSR1* were significantly increased solely in EpCAM$^-$/NCAM$^+$ cells without induction of neuroectodermal marker genes (*SOX1*, *NES*) (Figures 1F, S2B, and S2C). These findings were reproduced with the second hESC line, HUES8 (Figures S2D–S2F). Thus, CXCR4$^+$ cells represented highly purified DE cells, whereas sorted EpCAM$^-$/NCAM$^+$ cells represented purified ME cells.

### miRNA Profiling in Purified Endoderm, Purified Mesoderm, and hESCs

Sorted CXCR4$^+$ DE, EpCAM$^-$/NCAM$^+$ ME, and undifferentiated cells of the hESC line HUES8 were analyzed by qRT-PCR array cards (Figures 1B, 2A, and 2B). Out of the 754 tested miRNAs, 188 were not expressed in the analyzed populations, 369 were expressed in all populations, and 200 were expressed in two or only one population. Stringent criteria were used to identify differentially expressed miRNAs with a C_t value of <28 and an exclusive or a 10-fold altered expression compared with the other populations (Table 1 and Figures 2A and 2B).

According to these criteria 12 upregulated and 7 downregulated miRNAs were detected in the CXCR4$^+$ DE population (Table 1). miR489-3p was expressed in all populations but exhibited a strong induction (>44-fold) in DE cells, while miR-1263 was exclusively expressed in this population. In line with earlier studies, miR-375 (>100-fold) and the hESC-enriched miR-371-373 cluster were

---

(C) Representative flow-cytometric dot plot diagrams of HES3 cells in the undifferentiated state (ESC) or after 4 days of differentiation with the indicated protocols. Numbers represent the respective percentages of cells in the indicated quadrant. Depicted are CXCR4 and CD49e (upper panel) or EpCAM and NCAM (lower panel).

(D–F) Normalized expression of marker genes for pluripotency (*NANOG*, *POU5f1*, *SOX2*) (D), DE (*FOXA2*, *SOX17*, *GSC*) (E), and ME (*PDGFRA*, *KDR*, *CD34*) (F) scaled to hESC. Values are mean ± SEM, n = 4–7. ANOVA plus Bonferroni's post hoc test, *p < 0.05, **p < 0.01 compared with hESC. C$^-$, CXCR4$^-$ cells; C$^+$, CXCR4$^+$ cells; E$^+$N$^-$, EpCAM$^+$/NCAM$^-$ cells; E$^-$N$^+$, EpCAM$^-$/NCAM$^+$ cells.
See also Figures S1 and S2.
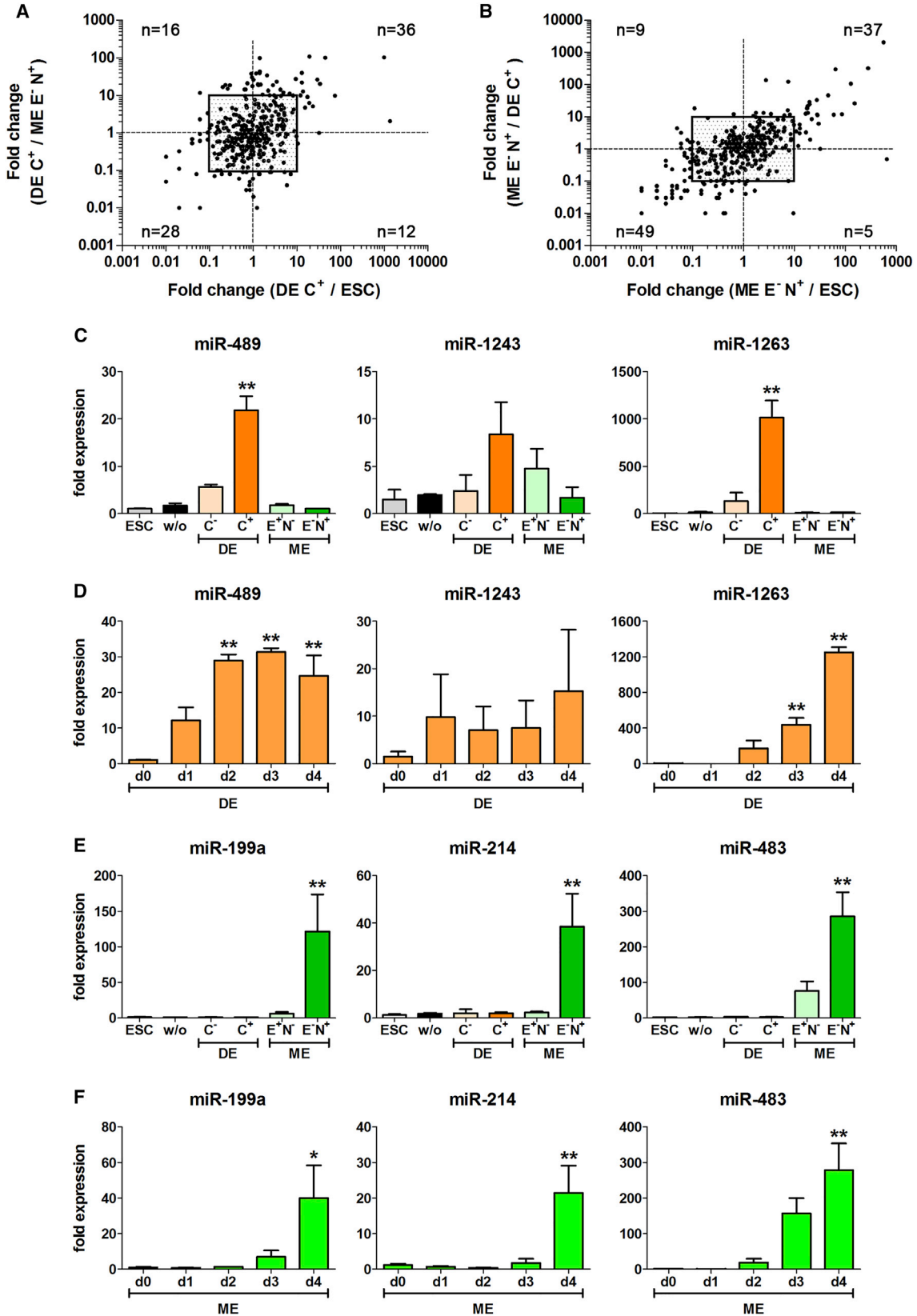
(legend on next page)

also upregulated in DE cells (Fogel et al., 2015; Hinton et al., 2010; Joglekar et al., 2009; Lakshmipathy et al., 2007; Laurent et al., 2008; Stadler et al., 2010). Similar to earlier results (Fogel et al., 2015; Hinton et al., 2014), three of the seven downregulated miRNAs are part of an miRNA cluster on chromosome 19 (miR-517a-3p, miR518e-3p, and miR-520g-3p), suggesting an inhibitory role of this cluster for DE development.

Sorted EpCAM$^-$/NCAM$^+$ ME cells exhibited 15 upregulated and 14 downregulated miRNAs compared with DE and ESCs according to our criteria (Table 1). Seven out of the 15 upregulated miRNAs showed either an exclusive or a more than 100-fold induced expression in ME. Interestingly, the 3p and 5p form of miR-483 were included in the list of upregulated miRNAs but only miR-483-3p showed an exclusive expression in sorted ME. Six out of the 14 downregulated miRNAs are part of the miR-302 cluster that is linked to hESCs and DE development (Leonardo et al., 2012; Rosa and Brivanlou, 2011; Rosa et al., 2009). Interestingly, the endodermal-enriched miR-489-3p is also in the list of repressed miRNAs, indicating its inverse regulation during DE and ME formation.

Validation of Endoderm- and Mesoderm-Specific miRNAs

For further validation we focused on top-ranked upregulated miRNAs (Table 1), and analyzed their expression in sorted populations and during differentiation using a second hESC line (HES3) to exclude cell-line-dependent effects.

The miRNAs miR-489-3p and miR-1263 were highly expressed only in CXCR4$^+$ DE cells, while miR-1243 could not be validated as endoderm specific (Figure 2C). Time-course analysis revealed that miR-489-3p was induced at day 1 and plateaued from day 2 on, whereas miR-1263 started to be increased from day 2 on and peaked at day 4 with a ∼40-fold stronger induction compared with miR-489-3p (Figure 2D). Thus, miR-489-3p might be important during early events of DE formation, whereas miR-1263 seems to be important for later stages. The miR-371-373 cluster was already described as hESC enriched (Lakshmi-

pathy et al., 2007; Laurent et al., 2008; Stadler et al., 2010), but CXCR4$^+$ DE cells exhibited even a ∼5-fold increased expression of this cluster compared with hESCs and all other populations (Figure S3A). Their expression was induced from day 2 on and plateaued (miR-372-3p) or peaked at day 4 (Figure S3B), indicating additional roles of these miRNAs during DE formation.

Mesodermal-enriched miRNAs with an exclusive or more than 100-fold induced expression in ME cells were chosen for further validation. Out of these seven miRNAs miR-199a-3p, miR-214-3p, and miR-483-3p showed a strong induction nearly exclusively in EpCAM$^-$/NCAM$^+$ ME cells (Figure 3E). Their expressions were detectable from day 2/3 on and significantly increased until day 4, with the strongest induction rate of more than 200-fold detected for miR-483-3p (Figure 3F). Expression of miR-143-3p and miR-145-5p was significantly induced in ME cells, whereas miR-10a-5p and miR-196b-5p were induced in ME cells and in the EpCAM$^+$/NCAM$^-$ population (Figures S3C and S3D). However, these four miRNAs were also induced by a treatment with CHIR alone (Figure S3E), suggesting that they are potentially regulated by Wnt/β-catenin signaling independent of the developmental stage.

miR-1263 and miR-489 Facilitate Endoderm Differentiation

Next, effects of the endoderm-specific miR-489-3p and miR-1263 on DE formation were analyzed by transfecting hESCs prior to differentiation (Figure 3A). Under optimal DE conditions (∼70% CXCR4$^+$ cells), transfection of miR-489-3p or miR-1263 mimic showed slightly increased numbers of CXCR4$^+$ cells at day 2, whereas at day 4 only miR-1263 mimic maintained this tendency with a ∼10% increased number of DE cells (Figure S4A). We also tested a suboptimal DE condition (2.5 μM CHIR instead of 5 μM for the first 24 hr) to assess the miRNA effect in a setting of less extrinsic signal strength (Figure 3B).

Under the suboptimal DE condition, transfection of miR-489-3p or miR-1263 mimic significantly increased the number of CXCR4$^+$ cells compared with the negative control (NC). This effect was especially more pronounced at

Figure 2. Comparative Analysis of the miRNomes (HUES8) and Validation of Selected miRNAs in a Second hESC Cell Line (HES3)
(A) Comparison of the miRNA expression ratios of purified DE cells versus ME cells (y axis) or versus hESCs (x axis) using the HUES8 line.
(B) miRNA expression ratios of ME cells versus DE cells (y axis) or versus hESCs (x axis) (HUES8 cell line). (A) and (B) present results from pooled samples each comprising 4 independent experiments. Plotted are the 369 miRNAs expressed in all analyzed populations. The central quadrant represents the chosen 10-fold altered expression difference and the indicated numbers represent the miRNAs in the respective quadrant.
(C–F) Normalized expressions of the indicated miRNAs in the different populations (C and E) or during DE (D) or ME (F) differentiation, respectively. Values are mean ± SEM, n = 4–8. ANOVA plus Bonferroni's post hoc test, *p < 0.05, **p < 0.01 compared with all other populations in (C) and (E), and compared with day 0 in (D) and (F). C$^+$, CXCR4$^+$ cells; E$^-$N$^+$, EpCAM$^-$/NCAM$^+$ cells; C$^-$, CXCR4$^-$ cells; E$^+$N$^-$, EpCAM$^+$/NCAM$^-$ cells.
See also Figure S3.

Table 1. Upregulated and Downregulated miRNAs in Differentiated Cells Compared with Undifferentiated Cells

Endoderm			Mesoderm		
	Fold Change of Expression			**Fold Change of Expression**	
miRNA	Compared with ESCs	Compared with ME	miRNA	Compared with ESCs	Compared with DE
Upregulated			**Upregulated**		
miR-1263	n.d. in ESC	n.d. in ME	miR-196b-5p	n.d. in ESC	n.d. in DE
miR-1243	1354.3	2.1	miR-483-3p	n.d. in ESC	n.d. in DE
miR-375	988.6	102.8	miR-675-5p	n.d. in ESC	n.d. in DE
miR-888-5p	74.6	9.7	miR-214-3p	1387.6	n.d. in DE
miR-489-3p	44.4	101.2	miR-10a-5p	563.9	2043.6
miR-371-3p	33.9	20.2	miR-199a-3p	281.5	320.2
miR-7-2-3p	29.3	26.3	miR-145-5p	129.3	105.6
miR-373-3p	19.2	6.3	miR-193-5p	64.4	300.0
miR-372-3p	17.5	9.1	miR-143-3p	57.2	n.d. in DE
miR-661	13.8	12.7	miR-483-5p	46.1	45.7
miR-200a-5p	9.4	27.3	miR-532-3p	28.5	11.0
miR-1260a	2.4	10.1	miR-455-3p	28.0	11.6
			miR-365-3p	20.0	24.4
			miR-15a-5p	18.4	13.2
			miR-362-5p	16.6	12.4
Downregulated			**Downregulated**		
miR-154-3p	n.d. in DE	n.d. in DE	miR-98-5p	n.d. in ME	n.d. in ME
miR-518e-3p	5.8×10^{-3}	5.5×10^{-2}	miR-367-3p	1.2×10^{-2}	6.0×10^{-2}
miR-187-3p	3.9×10^{-2}	6.7×10^{-1}	miR-302c-5p	1.2×10^{-2}	1.0×10^{-2}
miR-520g-3p	4.2×10^{-2}	5.3×10^{-2}	miR-302b-3p	2.4×10^{-2}	2.7×10^{-2}
miR-517a-3p	5.7×10^{-2}	6.0×10^{-2}	miR-302d-3p	3.0×10^{-2}	3.3×10^{-2}
miR-512-3p	5.8×10^{-2}	9.3×10^{-2}	miR-302d-5p	3.1×10^{-2}	2.6×10^{-2}
miR-100-5p	6.2×10^{-2}	8.1×10^{-3}	miR-302a-5p	3.3×10^{-2}	2.3×10^{-2}
			miR-200b-3p	3.9×10^{-2}	3.8×10^{-2}
			miR-302a-3p	5.4×10^{-2}	5.6×10^{-2}
			miR-31-5p	6.5×10^{-2}	5.1×10^{-2}
			miR-520c-3p	1.7×10^{-1}	7.5×10^{-2}
			miR-559	3.0×10^{-1}	2.9×10^{-2}
			miR-200a-5p	3.4×10^{-1}	3.7×10^{-2}
			miR-489-3p	4.4×10^{-1}	1.0×10^{-2}

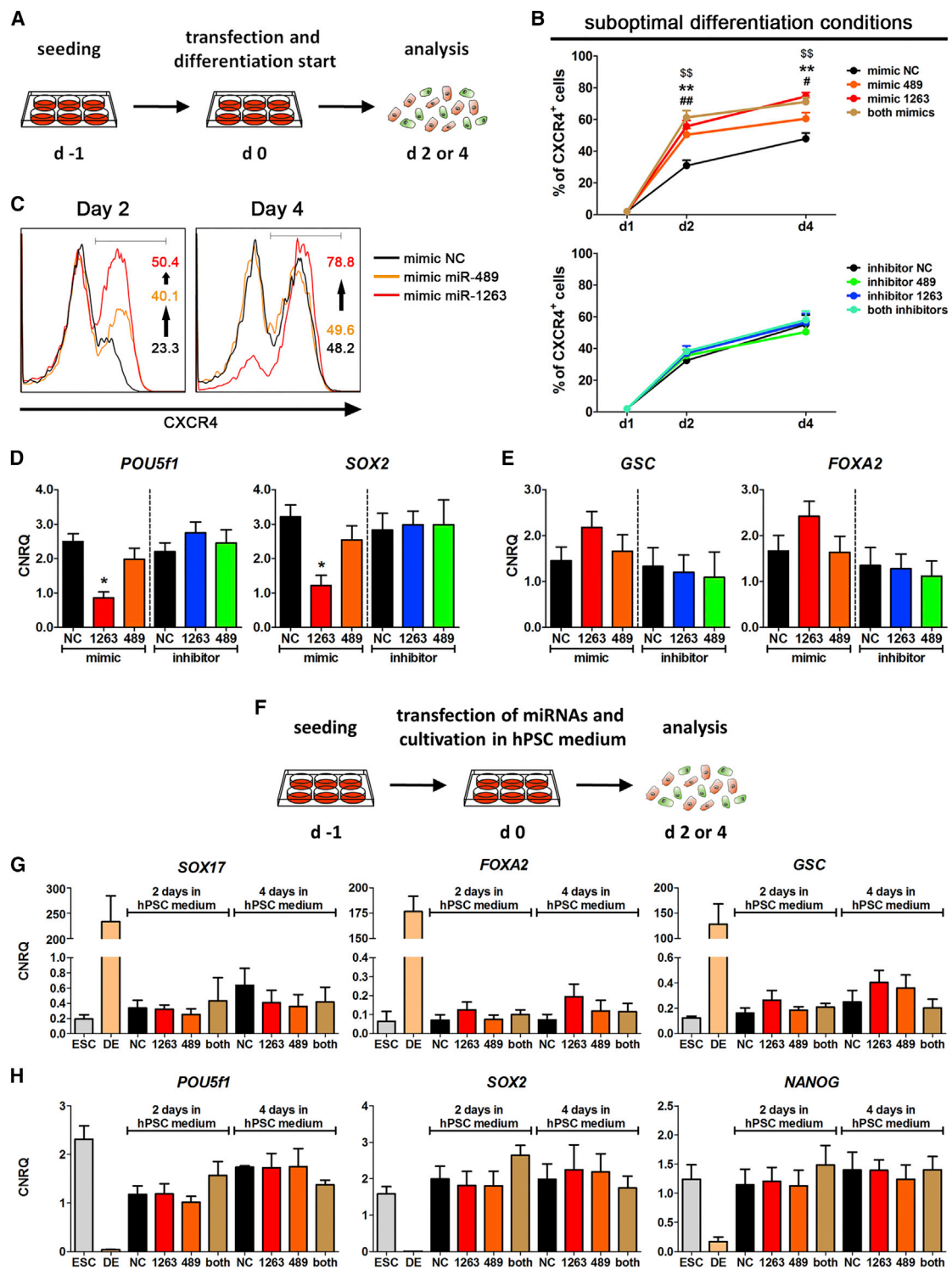n.d., not detected; DE, definitive endoderm; ME, mesoderm.

Figure 3. Functional Analysis of Endoderm-Specific miRNAs (HES3)

(A) Schematic overview of the transfection of miRNA mimics/inhibitors.

(B) Time courses of the derivation of CXCR4$^+$ cells during suboptimal DE differentiation after transfection with mimics or inhibitors. Values are mean ± SEM, n = 5–6. ANOVA plus Bonferroni's post hoc test, $^{\#}p < 0.05$ or $^{\#\#}p < 0.05$ (miR-489-3p), $^{**}p < 0.01$ (miR-1263), $^{\$\$}p < 0.05$ (both) compared with the negative control (NC) on day 2 or day 4, respectively.

(legend continued on next page)

day 4 for miR-1263 than for miR-489-3p (Figures 3B and 3C). Simultaneous transfection of both mimics did not further enhance the number of CXCR4$^+$ cells but showed a profile similar to that of miR-1263 alone (Figure 3B). Upon transfection with the miR-1263 mimic, pluripotency marker genes (*POU5f1*, *SOX2*, *NANOG*) were significantly downregulated at day 4 without affecting the extraembryonic endoderm marker *SOX7* (Figures 3D and S4B). Contrarily, the endodermal marker genes *GSC*, *MIXL1*, and *FOXA2* were slightly increased, while *SOX17* showed no differences (Figures 3E and S4C). Two days after transfection a slight but not significantly reduced expression of the pluripotency marker genes was detected, while all other genes showed no differences (Figure S4D). Interestingly, transfection of the respective miRNA inhibitors alone or together showed no effects on DE formation (Figures 3B–3E and S4A–S4D). Taken together, miR-1263 facilitates and accelerates DE differentiation while miR-489-3p promotes initial cell-fate decisions with a less pronounced effect on the overall efficiency compared with miR-1263.

Next, the effects of miR-489-3p and miR-1263 on hESCs were analyzed by transfecting their mimics alone or together followed by cultivation in hPSC medium (Figure 3F). Under this condition, transfection of the mimics alone or together did not induce the expression of primitive streak/DE marker genes (*SOX17*, *FOXA2*, *GSC*) or alter the expression of pluripotency marker genes (*POU5f1*, *SOX2*, *NANOG*) (Figures 3G and 3H). Thus, miR-489-3p and/or miR-1263 were not able to induce differentiation of hESCs under hPSC cultivation conditions.

Functional Characterization of Mesodermal miRNAs

Earlier publications demonstrated that KDR$^+$ cells represent lateral plate ME, whereas PDGFRA$^+$ cells exhibit a paraxial ME character (Sakurai et al., 2006; Tan et al., 2013). Thus, the distribution of these cells was analyzed in EpCAM$^-$/NCAM$^+$ cells upon transfection with mimics or inhibitors of identified ME-enriched miRNAs (Figure 4A). Inhibition of miR-483-3p significantly reduced the number of PDGFRA$^+$ cells, while inversely transfection of miR-483-3p mimic significantly increased their number compared with the respective NC (Figures 4B and 4C). Inhibiting or mimicking miR-199a-3p or miR-214-3p did not yield any significant changes (Figure 4C). Also, the number of KDR$^+$ cells was not altered under all tested conditions (Figure 4C). Transfection of a second hESC line (HUES8) with the miR-483-3p inhibitor or mimic resulted in nearly identical results (Figure 4D) excluding a cell-line-dependent effect. In line with these flow-cytometric results, inhibition of miR-483-3p significantly reduced the expression of *PDGFRA* while mimicking slightly increased *PDGFRA* expression without affecting *KDR* in both hESC lines (Figures 4E and S4E). Interestingly, the expression of *CD34* decreased significantly upon inhibition of miR-483-3p (Figures 4E and S4E). Thus, the observed changes of the PDGFRA$^+$ population upon miR-483-3p modulation were confirmed on the protein and mRNA levels (Figures 4C–4E and S4E), demonstrating an important role of miR-483-3p for the formation of PDGFRA$^+$ cells during ME development.

Next, the expression of miR-199a-3p, miR-214-3p, and miR-483-3p was analyzed in the different NCAM$^+$ subpopulations (Figures 4F and 4G). The miR-483-3p was already expressed in the PDGFRA$^-$ (P$^-$) population and increased in PDGFRA$^+$ (P$^+$) cells, whereas its expression was nearly abolished in CD34$^+$ cells (Figure 4G). Also miR-199a-3p and miR-214-3p were expressed in P$^-$ cells but their expression was passed to CD34$^+$ cells with a nearly absent expression in the P$^+$ population (Figure 4G). Taken together, all of these three miRNAs were already expressed in the P$^-$ population, which might contain a potential progenitor cell population for P$^+$ and CD34$^+$ cells. Furthermore, miR-483-3p was passed from the P$^-$ population to P$^+$ cells, whereas miR-199a-3p and miR-214-3p were nearly abolished in these cells but passed to the CD34$^+$ population.

Potential Candidate Genes and Their Functions during Differentiation

In silico prediction of potential miRNA binding sites in the 3′ UTR region of mRNAs was performed with the TargetScan and miRanda algorithms by choosing a total context^{++} score < −0.4 and a mirSVR score < −1.0 as cutoffs. For the endodermal miR-1263, 195 (TargetScan) and 102 (miRanda) potential targets were predicted with 39 overlapping targets (Figures 5A and 5B). *In silico* prediction for miR-483-3p revealed 19 (TargetScan) and 133 (miRanda) targets, with five candidates included in both predictions (Figures 5A and 5B). Target prediction for miR-199a-3p

(C) Representative flow-cytometric histograms of CXCR4 staining at days 2 and 4.
(D and E) Normalized expression of marker genes for pluripotency (*POU5f1*, *SOX2*) (D) and primitive streak/DE (*GSC*, *FOXA2*) (E) after 4 days of differentiation post transfection. Values are mean ± SEM, n = 5–6. ANOVA plus Bonferroni's post hoc test, *p < 0.05 compared with the respective NC.
(F) Schematic overview of the transfection of miRNA mimics/inhibitors under hESC cultivation condition.
(G and H) Normalized expression of marker genes for primitive streak/DE (*SOX17*, *FOXA2*, *GSC*) (G) and pluripotency (*POU5f1*, *SOX2*, *NANOG*) (H) 2 or 4 days after transfection and cultivation in hESC medium. Values are mean ± SEM, n = 4.
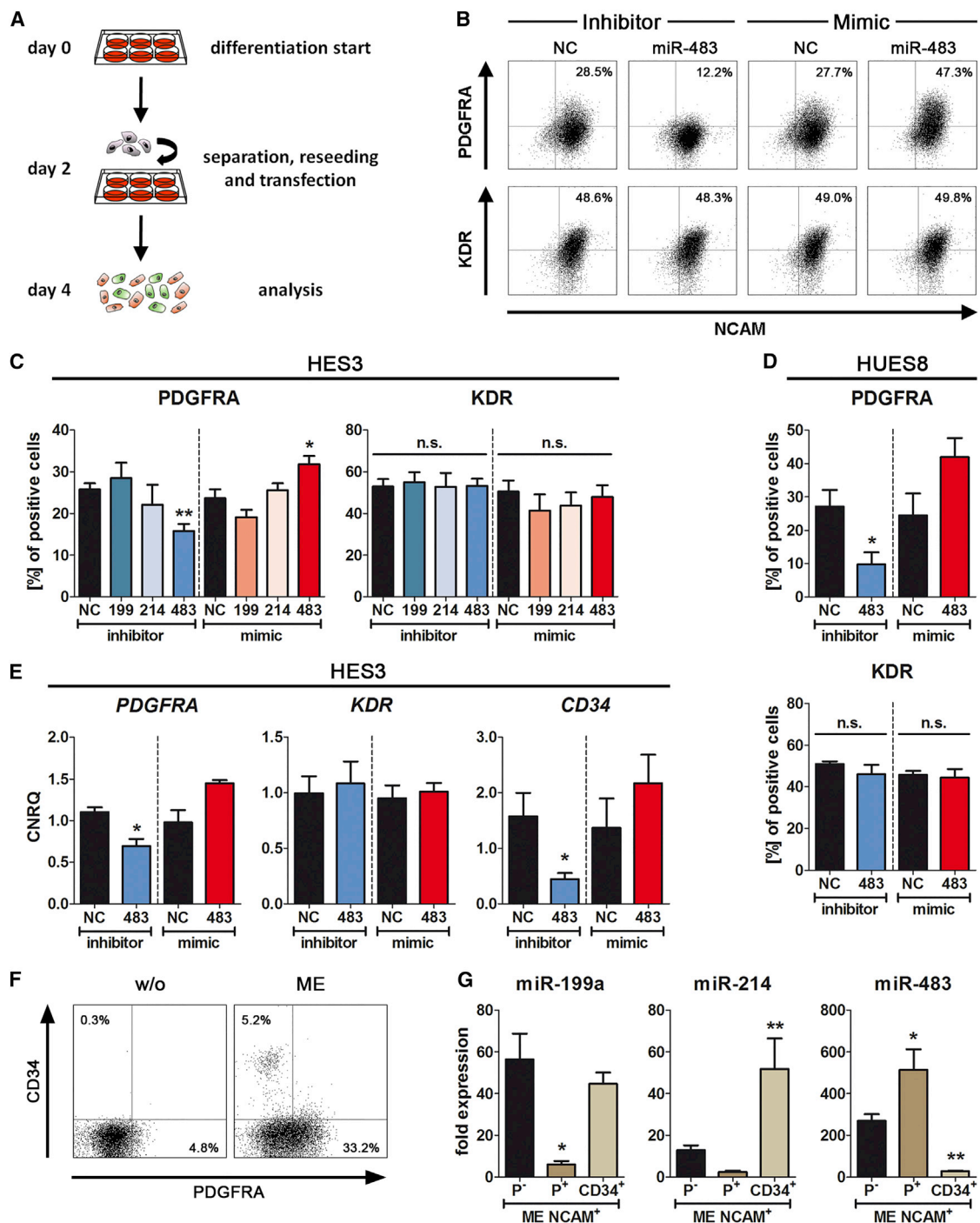See also Figures S4A–S4D.

Figure 4. Functional Analysis of Mesoderm-Specific miRNAs

(A) Schematic overview of the experimental setup.

(B) Representative flow-cytometric dot plot diagrams after 4 days of ME differentiation (HES3). Transfected miRNA inhibitors or mimics are marked. Indicated numbers represent the percentages of double-positive cells (upper panel: NCAM$^+$/PDGFRA$^+$; lower panel: NCAM$^+$/KDR$^+$).

(C and D) Quantification of NCAM$^+$/PDGFRA$^+$ and NCAM$^+$/KDR$^+$ cells by flow cytometry at day 4 using the HES3 (C) or HUES8 (D) cell line. Transfection with the indicated mimics/inhibitors was performed at day 2. Values are mean ± SEM, n = 4–8. ANOVA plus Dunnett's post hoc test compared with the respective NC (C) or Student's t test (D), *p < 0.05 and **p < 0.01; n.s., not significant.

(legend continued on next page)

and miR-214-3p resulted in an overlap of 29 and 25 potential targets, respectively (Figures S5A–S5D).

Of the predicted targets for miR-1263, *KLF4*, a regulator for pluripotency, exhibited one potential binding site in its 3′ UTR. Combined transfection of a luciferase reporter vector and miR-1263 mimic strongly repressed luciferase activity (Figure 5C), indicating binding to this site. Of the predicted targets for miR-483-3p, phosphoglycerate mutase 1 (*PGAM1*) contained two potential binding sites and binding of miR-483-3p was demonstrated with the luciferase reporter assay (Figure 5C). Interestingly, the so far less characterized gene zinc finger and BTB domain-containing 26 (*ZBTB26*) was proved as a target of miR-1263 and miR-483-3p (Figure 5C), indicating a negative influence of this gene on DE and ME differentiation. The activin A receptor type 2A (*ACVR2A*) was determined as a possible target of miR-199a-3p, while N-α-acetyltransferase 15 (*NAA15*) is a potential target of miR-214-3p and miR-1263 according to the luciferase assay results (Figure S5E).

Next, changes of the KLF4 and PGAM1 protein expression after transfection with the respective miRNA mimics were examined. For this purpose HEK293 cells were used as a model cell line because these cells had a similar expression of KLF4 and PGAM1 on the mRNA and protein levels compared with hESCs (HES3) and a nearly undetectable expression of miR-1263 and miR-483-3p (Figures S5F–S5I). The transfection of miR-1263 mimic significantly decreased KLF4 protein levels 24 hr and 48 hr post transfection compared with the respective NC (Figure 5D). Also, transfection of the miR-483-3p mimic was able to significantly decrease the protein amount of PGAM1 at both time points compared with the NC (Figure 5E).

Surprisingly, the mRNA expression of *KLF4* in sorted CXCR4^{+} DE cells was comparable with that of hESCs (Figure 6A). Certainly the KLF4 protein expression significantly decreased upon differentiation, and transfection of the miR-1263 mimic further decreased the KLF4 protein amount compared with the NC (Figure 6B). Inversely to the amount of KLF4 protein, the number of CXCR4^{+} DE cells increased (Figures 6B and 6C), suggesting that lower KLF4 protein levels are beneficial for DE formation. Inhibition of miR-1263 had no effects on the differentiation efficiency into the DE and the amount of KLF4 protein was maintained on the same level as the NC

(Figures 3B, S4A, and S6). We speculate that the amount of inhibitor may not be able to quench the strong miR-1263 expression.

To further examine the influence of KLF4 on DE formation, we transfected siRNA prior to suboptimal DE differentiation. This resulted in a ∼50% decrease of the *KLF4* gene expression (Figure 6D) and, confirmatory to the mimic transfections, in a significant increase of CXCR4^{+} cells compared with the NC (Figures 6E and 6F). Thus, downregulation of KLF4 alone increased the overall differentiation efficiency but did not accelerate DE formation.

To elucidate potential roles of the miR-483-3p target PGAM1 during ME differentiation, we performed transfection of siRNA. This reduced the gene expression of *PGAM1* by ∼50% at day 5 (Figure 6G) and resulted in a small but significant induction of PDGFRA^{+} cells compared with the NC, without effects on the gene expression of *KDR* or *PDGFRA* (Figures 6H and 6I).

DISCUSSION

One of the earliest cell-fate decisions during development is the formation of the three embryonic germ layers. The study of human development using hPSCs represents a promising *in vitro* model. Although many signaling pathways are known that contribute to *in vitro* germ layer formation, the differentiation yields are often inefficient and variable. Next to gene regulatory networks, miRNAs have the potential to influence cell-fate decisions (Kanellopoulou et al., 2005; Rosa et al., 2009; Wang et al., 2007) by fine-tuning the expression of their target genes on the post-transcriptional level (Bartel, 2009). In this report three different embryonic populations were analyzed to study the differential expression of miRNAs and their functions during gastrulation. In contrast to previous reports (Fogel et al., 2015; Hinton et al., 2010, 2014; Liao et al., 2013), purified DE and ME populations were compared with hESCs to exclude unwanted cell lineages. This permitted a distinct correlation of miRNA expression to a specific cell fate.

DE differentiation was performed using an established protocol (Diekmann et al., 2015). For ME induction different conditions were tested, and subsequently a

(E) Normalized gene expressions of ME markers (*PDGFRA, KDR, CD34*) at day 4 (HES3). Values are means ± SEM, n = 4. Student's t test, *p < 0.05.

(F) Depicted is a PDGFRA and CD34 staining of the mesodermal NCAM[+] population at day 4 after randomized or ME differentiation (HES3). Indicated percentages represent the numbers of cells within the quadrant of this particular experiment.

(G) Normalized miRNA expression in the three purified populations of mesodermal NCAM^{+} cells scaled to undifferentiated hESCs (HES3). Values are mean ± SEM, n = 3–6. ANOVA plus Bonferroni's post hoc test, *p < 0.05 and **p < 0.01 compared with P^{−} cells. P^{−}, NCAM^{+}/PDGFRA^{−}/CD34^{−} cells; P^{+}, NCAM^{+}/PDGFRA^{+}/CD34^{−} cells; CD34^{+}, NCAM^{+}/CD34^{+}/PDGFRA^{−} cells.

See also Figure S4E.

A In Silico Predicted Targets

miR-1263

156 | 39 | 63
TargetScan — miRanda

miR-483-3p

14 | 5 | 128
TargetScan — miRanda

B

		miR-1263		*miR-483-3p*
ALKBH2	DNAH8	MAP3K2	SNAP91	C5orf42
ARMC2	EFNA3	MTHFD2	STX16	ODF2
ATAD2	FBXO11	MTMR2	TASP1	**PGAM1**
ATP10A	GBE1	**NAA15**	TCEAL8	WDR44
C11orf87	GPKOW	NAA30	TMEM136	**ZBTB26**
CDH8	KCTD16	RAB39B	TOMM20L	
CEP97	**KLF4**	SGK3	TRMT6	
CSGALNACT2	LRRTM1	SLC25A13	WDR41	
DCUN1D4	LYPD1	SLC35F3	**ZBTB26**	
DIXDC1	MAN2A1	SLC38A2		

C KLF4 PGAM1 ZBTB26

D KLF4

E PGAM1

Figure 5. Target Prediction and Verification of Their Regulation via Endoderm- and Mesoderm-Specific miRNAs

(A) Predicted targets of miR-1263 and miR-483-3p calculated by the TargetScan or miRanda algorithm.

protocol was used that is similar to that of Tan et al. (2013). Specific expression of surface proteins was used to purify the desired cell populations from heterogeneously composed differentiation cultures. Pure DE cells were obtained using the specific DE marker CXCR4 (Davenport et al., 2016; Diekmann and Naujok, 2016; Kroon et al., 2008; Naujok et al., 2014). In contrast to a recent publication (Wang et al., 2011), CD49e could not be validated as truly DE specific because it was also detectable upon ME differentiation. In line with Evseenko et al. (2010), the EpCAM$^-$/NCAM$^+$ population represented early ME cells. Additionally, we showed that EpCAM was passed from hPSCs to the DE but not to ME cells. Thus, EpCAM could be an additional surface marker to distinguish DE from ME.

Analysis of the specific miRNomes from purified populations and hESCs identified differentially expressed miRNAs, from which some were already described. The DE-associated miR-375 (Fogel et al., 2015; Hinton et al., 2010, 2014; Joglekar et al., 2009; Liao et al., 2013) was highly enriched in purified DE cells and served as positive control for our purification and characterization strategy. Earlier studies associated the miR-371-373 cluster with the pluripotent state (Lakshmipathy et al., 2007; Laurent et al., 2008; Stadler et al., 2010), while recent reports showed its upregulation also in heterogeneously composed DE populations (Fogel et al., 2015; Hinton et al., 2010, 2014; Liao et al., 2013). Here we verified that this cluster is upregulated specifically in DE cells. Thus, the miR-371-373 cluster is important for the maintenance of pluripotency and also for proper DE development. This might be mediated by modulation of the Nodal/transforming growth factor β (TGF-β) signaling, similar to the miR-302/367 cluster (Rosa et al., 2009, 2014; Barroso-delJesus et al., 2011).

Recently, miR-489-3p and miR-1263 were described to be upregulated in mixed DE populations, but these reports did

(B) Tabular presentation of the candidate genes predicted by both algorithms for miR-1263 and miR-483-3p. Names written in bold were experimentally analyzed by luciferase reporter assays.

(C) Luciferase activity normalized to the β-galactosidase activity for the subcloned 3′ UTRs of *KLF4*, *PGAM1*, and *ZBTB26* in HEK293 cells upon transfection of the indicated mimics and the reporter plasmids. Values are mean ± SEM, n = 4–6. Two-tailed Student's t test, **p < 0.01.

(D and E) Normalized protein expression of KLF4 (D) and PGAM1 (E) 24 hr and 48 hr post transfection with the indicated miRNA mimics in HEK293. The NC of each experiment was set as 100%. For each protein one representative western blots is shown on the right. Values are mean ± SEM, n = 4–5. ANOVA plus Bonferroni's post hoc test, *p < 0.05 and **p < 0.01 compared with the respective NC. See also Figure S5.
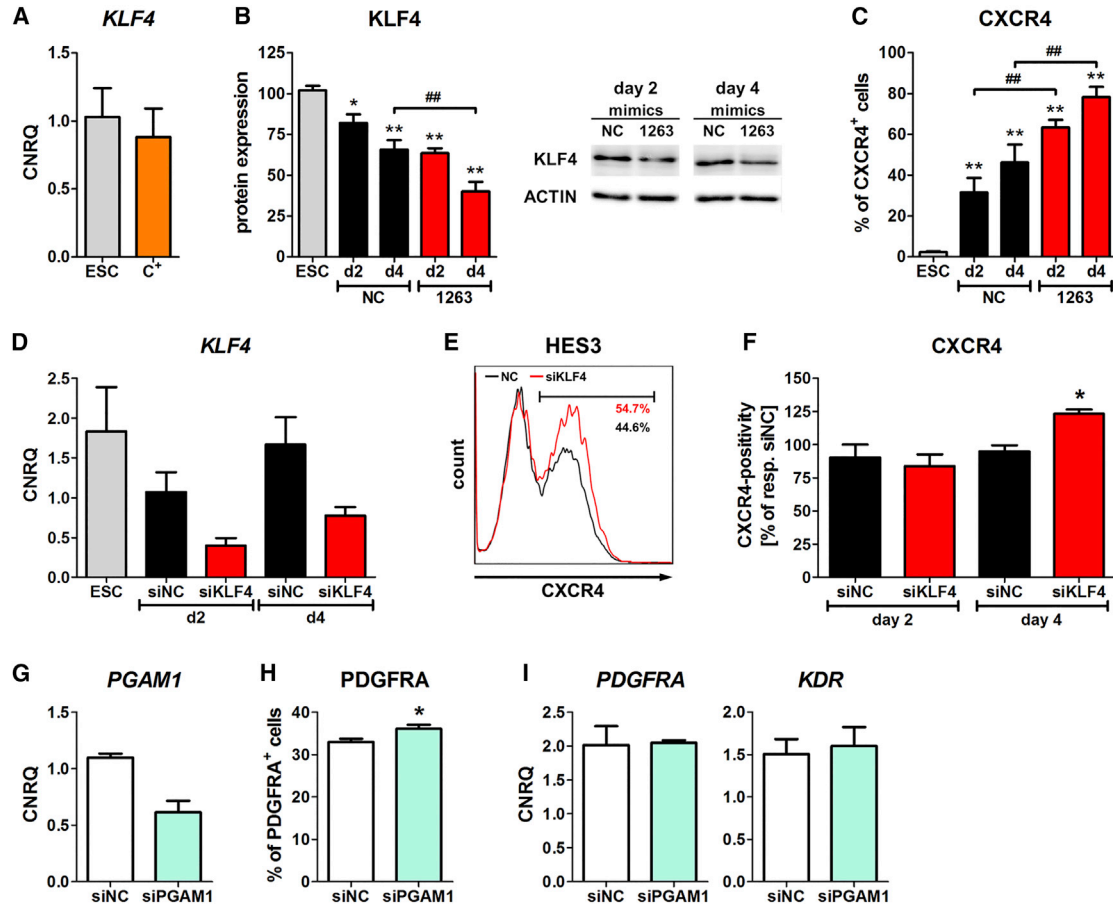
Figure 6. Influence of KLF4 and PGAM1 on Endoderm or Mesoderm Differentiation (HES3)

(A) Normalized gene expression of *KLF4* in undifferentiated hESCs (HES3) and sorted CXCR4^{+} DE cells. Values are mean ± SEM, n = 4.

(B and C) Normalized protein expression of KLF4 (B) and quantification of CXCR4^{+} DE cells by flow cytometry (C) after suboptimal DE differentiation and transfection with the indicated miRNA mimics (HES3). Values are mean ± SEM, n = 4. ANOVA plus Bonferroni's post hoc test, *p < 0.05, **p < 0.01 compared with hESCs and ##p < 0.01 between miR-1263 and the NC on the particular day. A representative western blot of KLF4 is depicted in (B).

(D) Normalized gene expression of *KLF4* in hESCs and after transfection with the indicated siRNAs plus subsequent suboptimal DE differentiation. Values are mean ± SEM, n = 4–6.

(E and F) Representative flow-cytometric histogram of CXCR4^{+} cells at day 4 (E) and quantification of CXCR4^{+} cells at days 2 and 4 (F) upon siRNA transfection and subsequent suboptimal DE differentiation. Values in (F) are mean ± SEM and one respective NC of each experiment is scaled to 100%, n = 4–6. Student's t test, *p < 0.05.

(G–I) Normalized gene expression of *PGAM1* (G), flow-cytometric quantification of PDGFRA^{+} cells (H), and normalized gene expression of *PDGFRA* and *KDR* (I) at day 5 of ME differentiation. The cells were reseeded on day 2 and transfected with the indicated siRNAs. Values are mean ± SEM, n = 4–6. Student's t test, *p < 0.05.

See also Figure S6.

not characterize their specific functions (Liao et al., 2013; Fogel et al., 2015; Hinton et al., 2014). In this study we confirmed their specific expression in DE cells. Functional characterization demonstrated that both miRNAs accelerated and increased DE formation. However, miR-1263 was more effective in increasing the overall DE efficiency. Simultaneous transfection of both miRNA mimics showed a profile similar to that of the miR-1263 mimic alone, sug-gesting that the effect on the overall DE efficiency is predominantly mediated by miR-1263. However, both miRNAs under hPSC cultivation conditions were not potent enough alone or together to induce differentiation by themselves. *In silico* target prediction and functional evaluation confirmed *KLF4*, among others, as a target mRNA of miR-1263, which is regulated also on the protein level. Interestingly, *KLF4* was expressed in hESCs and

purified DE cells on a similar level, but downregulation of the KLF4 protein correlated with a more efficient DE formation. This effect could be partially mimicked by siRNA-mediated downregulation of *KLF4*, albeit without accelerating DE formation. Thus, miR-1263 mediates its positive effects on DE formation partially by destabilization of the pluripotency transcriptional network via KLF4 downregulation. The comparison of the siRNA- and miR mimic-mediated effects suggests that other miR-1263 target genes are also involved in this process. Future studies should address the effects of further miR-1263 targets.

Our characterization of the identified ME-enriched miRNAs revealed different roles during ME formation. miR-199a-3p, miR-214-3p, and miR-483-3p were validated as miRNAs that may influence ME development or specification due to their strong induction and nearly exclusive expression in EpCAM⁻/NCAM⁺ ME cells. Even though miR-143-3p and miR-145-5p were exclusively expressed in purified ME cells, these two miRNAs, like miR-10a-5p and miR-196b-5p, were also induced upon CHIR treatment alone. A recent publication strengthens a potential role of miR-145 for ME formation because its overexpression inhibits hESC self-renewal and induces differentiation with an increased expression of ME and ectodermal genes (Xu et al., 2009). However, our data also suggest that these four miRNAs are potentially regulated by Wnt/β-catenin signaling independent of the developmental stage or that they might be expressed in a different ME sublineage induced by treatment with CHIR alone (Mendjan et al., 2014; Lian et al., 2013).

The early hPSC-derived ME can be subdivided into paraxial (PDGFRA⁺/CD34⁻) and lateral plate (KDR⁺/CD34⁺) ME (Tan et al., 2013). Here we provide evidence that miR-483-3p modulates the number of PDGFRA⁺ paraxial ME cells without affecting the number of KDR⁺ cells. In contrast, miR-199a-3p and miR-214-3p showed no effects on these two ME subpopulations although they may have functions in the PGFRA⁻ ME sublineages. This is indicated by their maintained/increased expression in the CD34⁺ population, while being nearly abolished in the PGFRA⁺ paraxial ME lineage. We speculate that the two analyzed ME populations arise from an exclusively NCAM⁺ ancestor that serves as progenitor pool. In the NCAM⁺ cells all three miRNAs were expressed, suggesting additional functions for all three miRNAs already in the early ME progenitor pool. Consequently, this report identified miR-483-3p as an important regulator of the PDGFRA⁺ paraxial ME that is capable of further differentiation into chondrocytes, osteocytes, and myocytes (Tan et al., 2013; Evseenko et al., 2010). All three miRNAs seem to be important for the NCAM⁺ population.

Target predication and experimental validation identified *PGAM1* as a target gene of miR-483-3p that is regulated on the mRNA and protein levels. Inhibition of *PGAM1* by siRNA could partially mimic the effect of miR-483-3p. Nonetheless it is likely that additional genes are regulated by this miRNA, which results in the more potent effect of miR-483-3p compared with the siRNA-mediated *PGAM1* reduction. *PGAM1* is part of the glycolysis pathway, which indicates a role of metabolic flux regulation to influence cell-fate decisions. This is in line with a recent publication showing that PSCs exhibited a higher glycolytic flux than early differentiated cells and that inhibition of glycolysis in PSCs leads to differentiation and histone deacetylation (Moussaieff et al., 2015).

Faial et al. (2015) showed that induction of ME genes required BMP4 signaling or Nodal/TGF-β antagonism, while upregulation of DE genes was strictly dependent on Nodal/TGF-β signaling. In this study we also functionally validated the type-2 activin receptor *ACVR2A* as target of the mesodermal miR-199a-3p, which is important for Nodal/TGF-β signaling. Together with the verified downregulation of the Nodal/TGF-β-regulating miR-302 cluster (Rosa et al., 2009; Barroso-delJesus et al., 2011), this suggests that miRNAs lower Nodal/TGF-β signaling to permit ME differentiation. Finally, we identified that miRNAs enriched either in DE or ME share identical target mRNAs as shown here for *ZBTB26* and *NAA15*. Both genes were not yet described to be functionally relevant for DE or ME specification, but both germ layers repressed these two genes. This raises the question of whether these unknown genes might be inhibitory for DE and ME differentiation or even for gastrulation. Further experiments will be needed to uncover these mechanisms.

In summary, this comprehensive analysis of purified DE and ME permitted the correlation of miRNA expression to particular cell fates. We found 12 upregulated and 7 down-regulated DE-specific miRNAs as well as 15 upregulated and 14 downregulated ME-specific miRNAs to match stringent criteria. The ME-enriched miR-199a-3p, miR-214-3p, and miR-483-3p seem to have functions already within the early ME progenitor pool, while miR-483-3p is additionally an important regulator for the development of PDGFRA⁺ paraxial ME cells. The miR-483-3p mediates its effects on the formation of PDGFRA⁺ cells in part by regulating PGAM1. In the DE population miR-489-3p and miR-1263 were validated as highly enriched. Both miRNAs could accelerate and increase the efficiency of DE differentiation upon overexpression, while the effect on the overall DE efficiency was predominantly mediated by miR-1263. *KLF4* was validated as a functional target of miR-1263, and siRNA-mediated downregulation of KLF4 mimicked the miR-1263 effect to some extent. This demonstrates that miR-1263 mediates its effects by interference with the pluripotent transcriptional network, although other targets will likely play a role.

EXPERIMENTAL PROCEDURES

For more detailed information of the experimental procedures and the used antibodies, please refer to Supplemental Experimental Procedures.

Human ESC Culture and Differentiation

HUES8 and HES3 cells were cultivated under feeder-free conditions and the differentiation was induced from a defined number of seeded singe cells as described earlier (Diekmann et al., 2015; Diekmann and Naujok, 2016; Naujok et al., 2014). Advanced RPMI-1640 supplemented with 1% penicillin-streptomycin, 1% Glutamax, and 0.2% fetal bovine serum was used as base medium and for randomized differentiation. DE differentiation was performed with 50 ng/mL activin A (Peprotech) and 5 μM (optimal condition) or 2.5 μM (suboptimal DE condition) CHIR (Cayman Chemicals) for 24 hr followed by 72 hr in the same medium without CHIR. Induction of ME differentiation was performed in base medium supplemented with 25 ng/mL BMP4 (Peprotech) plus 5 μM CHIR for 24 hr and subsequently for 72 hr in the same medium without CHIR. Media were changed daily during differentiation.

Flow Cytometry and Cell Sorting

Cells were washed, dissociated with trypsin/EDTA, resuspended in PBS plus 2% fetal calf serum, and counted. They were then stained with primary conjugated antibodies following standard protocols and measured on a CyFlow ML flow cytometer (Partec) or sorted at the central cell sorting facility of Hannover Medical School. Data analysis was performed with FlowJo.

Gene and miRNA Expression Analysis

Total RNA was isolated using the peqGOLD RNAPure kit (Peqlab) and total RNA plus small RNAs using the miRNeasy kit (Qiagen) following the manufacturer's instructions. From 1 to 2 μg total RNA cDNA was synthesized and subsequently 5–10 ng was used for each qRT-PCR reaction. Samples were measured in triplicates using specific primer pairs or TaqMan assays (Table S1) on a ViiA7 system (Thermo Fisher Scientific). Data normalization was performed with qBasePlus (Biogazelle) against the geometric mean of three stably expressed housekeeping genes (*G6PD*, *TBP*, *TUBA1A*; M < 0.5).

Reverse transcription for miRNA expression analysis was performed with either 25 ng (single miRNA assays) or 500 ng (array cards) of total RNA plus small RNAs. Sequence-specific primers (Table S2) or the respective Megaplex RT primer pools (array cards, Thermo Fisher Scientific) were used. For miRNA array cards, each analyzed population was a pooled sample from four independent experiments. Data normalization of single miRNA assays was performed with qBasePlus against three stably expressed controls (RNU48, U6 snRNA, mir-425-5p; M < 0.5) and for the array cards using the modified global mean normalization strategy (D'Haene et al., 2012).

miRNA and siRNA Transfection Experiments

For transfection of miRNA inhibitors/mimics (Thermo Fisher Scientific), Lipofectamine 2000 was used. Transfection during DE differentiation was performed on day 0 (30 pmol/24-well) directly af-

ter changing to the first DE medium. During ME differentiation, transfection with 30 pmol miRNA inhibitors/mimics per 12-well was performed on day 2 upon dissociation and reseeding (7.5 × 10^4 cells/cm^2) of the cells in ME differentiation medium plus 10 μM Y-27632 (Selleck Chemicals) to ensure acceptable transfection efficiencies. Transfection of siRNAs (Thermo Fisher Scientific) was performed accordingly using 50 pmol or 30 pmol per 12-well during DE or ME differentiation, respectively. Transfection efficiencies were examined by flow cytometry 24 hr later with an FAM-conjugated NC, and a 60% cutoff was set for further analysis.

Luciferase Reporter Assay

Partial 3′ UTRs harboring at least one potential binding site for the respective miRNA were individually cloned into the pMIR-REPORT vector (Thermo Fisher Scientific). Lipofectamine 2000 was used to co-transfect 20 ng of pMIR-REPORT, 20 ng of β-galactosidase control plasmid (Promega), and 30 nM miRNA mimic or control into HEK293 cells. After 24 hr, luciferase and β-galactosidase activity were measured (Promega) and normalization was performed against the β-galactosidase activity of the respective sample.

Western Blot

Cells were detached, collected, centrifuged, and resuspended in RIPA buffer (Thermo Fisher Scientific). These whole-cell extracts were sonicated and a protease inhibitor mixture (Roche Diagnostic) was added. The protein content was determined by BCA assay (Thermo Fisher Scientific). Ten to twenty micrograms of total protein were separated by SDS-PAGE and transferred via electro-blotting to a PVDF membrane. Blocking was performed with 2%–5% nonfat dry milk in PBS plus 0.1% Tween 20. Primary antibodies were incubated overnight at 4°C and subsequently washed and incubated with the respective peroxidase-labeled secondary antibodies. The bands were visualized by chemiluminescence using the ECL select or ECL detection kit (GE Healthcare Europe) on a chemiluminescence imager (INTAS Science Imaging). Densitometric analysis was performed with Image Studio Lite software (LI-COR).

Statistics

Unless stated otherwise, all data values represent mean ± SEM. The number of independent experiments (n) is stated in each figure legend. Statistical analyses were performed using GraphPad Prism software.

SUPPLEMENTAL INFORMATION

Supplemental Information includes Supplemental Experimental Procedures, six figures, and two tables and can be found with this article online at https://doi.org/10.1016/j.stemcr.2017.10.011.

REFERENCES

Barroso-delJesus, A., Lucena-Aguilar, G., Sanchez, L., Ligero, G., Gutierrez-Aranda, I., and Menendez, P. (2011). The Nodal inhibitor Lefty is negatively modulated by the microRNA miR-302 in human embryonic stem cells. FASEB J. 25, 1497–1508.

Bartel, D.P. (2009). MicroRNAs: target recognition and regulatory functions. Cell 136, 215–233.

Bernstein, E., Kim, S.Y., Carmell, M.A., Murchison, E.P., Alcorn, H., Li, M.Z., Mills, A.A., Elledge, S.J., Anderson, K.V., and Hannon, G.J. (2003). Dicer is essential for mouse development. Nat. Genet. 35, 215–217.

Chen, C., Ridzon, D., Lee, C.T., Blake, J., Sun, Y., and Strauss, W.M. (2007). Defining embryonic stem cell identity using differentiation-related microRNAs and their potential targets. Mamm. Genome 18, 316–327.

D'Haene, B., Mestdagh, P., Hellemans, J., and Vandesompele, J. (2012). miRNA expression profiling: from reference genes to global mean normalization. Methods Mol. Biol. 822, 261–272.

Davenport, C., Diekmann, U., Budde, I., Detering, N., and Naujok, O. (2016). Anterior-posterior patterning of definitive endoderm generated from human embryonic stem cells depends on the differential signaling of retinoic acid, Wnt-, and BMP-signaling. Stem Cells 34, 2635–2647.

Diekmann, U., Elsner, M., Fiedler, J., Thum, T., Lenzen, S., and Naujok, O. (2013). MicroRNA target sites as genetic tools to enhance promoter-reporter specificity for the purification of pancreatic progenitor cells from differentiated embryonic stem cells. Stem Cell Rev. 9, 555–568.

Diekmann, U., Lenzen, S., and Naujok, O. (2015). A reliable and efficient protocol for human pluripotent stem cell differentiation into the definitive endoderm based on dispersed single cells. Stem Cells Dev. 24, 190–204.

Diekmann, U., and Naujok, O. (2016). Generation and purification of definitive endoderm cells generated from pluripotent stem cells. Methods Mol. Biol. 1341, 157–172.

Eliasson, L., and Esguerra, J.L. (2014). Role of non-coding RNAs in pancreatic beta-cell development and physiology. Acta Physiol. 211, 273–284.

Evseenko, D., Zhu, Y., Schenke-Layland, K., Kuo, J., Latour, B., Ge, S., Scholes, J., Dravid, G., Li, X., MacLellan, W.R., et al. (2010). Mapping the first stages of mesoderm commitment during differentiation of human embryonic stem cells. Proc. Natl. Acad. Sci. USA 107, 13742–13747.

Faial, T., Bernardo, A.S., Mendjan, S., Diamanti, E., Ortmann, D., Gentsch, G.E., Mascetti, V.L., Trotter, M.W., Smith, J.C., and Pedersen, R.A. (2015). Brachyury and SMAD signalling collaboratively orchestrate distinct mesoderm and endoderm gene regulatory networks in differentiating human embryonic stem cells. Development 142, 2121–2135.

Fiedler, J., Batkai, S., and Thum, T. (2014). MicroRNA-based therapy in cardiology. Herz 39, 194–200.

Fogel, G.B., Kai, Z.S., Zargar, S., Hinton, A., Jones, G.A., Wong, A.S., Ficici, S.G., Lopez, A.D., and King, C.C. (2015). MicroRNA dynamics during human embryonic stem cell differentiation to pancreatic endoderm. Gene 574, 359–370.

Hinton, A., Afrikanova, I., Wilson, M., King, C.C., Maurer, B., Yeo, G.W., Hayek, A., and Pasquinelli, A.E. (2010). A distinct microRNA signature for definitive endoderm derived from human embryonic stem cells. Stem Cells Dev. 19, 797–807.

Hinton, A., Hunter, S.E., Afrikanova, I., Jones, G.A., Lopez, A.D., Fogel, G.B., Hayek, A., and King, C.C. (2014). sRNA-seq analysis of human embryonic stem cells and definitive endoderm reveals differentially expressed microRNAs and novel IsomiRs with distinct targets. Stem Cells 32, 2360–2372.

Joglekar, M.V., Joglekar, V.M., and Hardikar, A.A. (2009). Expression of islet-specific microRNAs during human pancreatic development. Gene Expr. Patterns 9, 109–113.

Kanellopoulou, C., Muljo, S.A., Kung, A.L., Ganesan, S., Drapkin, R., Jenuwein, T., Livingston, D.M., and Rajewsky, K. (2005). Dicer-deficient mouse embryonic stem cells are defective in differentiation and centromeric silencing. Genes Dev. 19, 489–501.

Kroon, E., Martinson, L.A., Kadoya, K., Bang, A.G., Kelly, O.G., Eliazer, S., Young, H., Richardson, M., Smart, N.G., Cunningham, J., et al. (2008). Pancreatic endoderm derived from human embryonic stem cells generates glucose-responsive insulin-secreting cells in vivo. Nat. Biotechnol. 26, 443–452.

Lakshmipathy, U., Davila, J., and Hart, R.P. (2010). miRNA in pluripotent stem cells. Regen. Med. 5, 545–555.

Lakshmipathy, U., Love, B., Goff, L.A., Jornsten, R., Graichen, R., Hart, R.P., and Chesnut, J.D. (2007). MicroRNA expression pattern of undifferentiated and differentiated human embryonic stem cells. Stem Cells Dev. 16, 1003–1016.

Laurent, L.C., Chen, J., Ulitsky, I., Mueller, F.J., Lu, C., Shamir, R., Fan, J.B., and Loring, J.F. (2008). Comprehensive microRNA profiling reveals a unique human embryonic stem cell signature dominated by a single seed sequence. Stem Cells 26, 1506–1516.

Leonardo, T.R., Schultheisz, H.L., Loring, J.F., and Laurent, L.C. (2012). The functions of microRNAs in pluripotency and reprogramming. Nat. Cell Biol. 14, 1114–1121.

Lian, X., Zhang, J., Azarin, S.M., Zhu, K., Hazeltine, L.B., Bao, X., Hsiao, C., Kamp, T.J., and Palecek, S.P. (2013). Directed cardiomyocyte differentiation from human pluripotent stem cells by modulating Wnt/beta-catenin signaling under fully defined conditions. Nat. Protoc. *8*, 162–175.

Liao, X., Xue, H., Wang, Y.C., Nazor, K.L., Guo, S., Trivedi, N., Peterson, S.E., Liu, Y., Loring, J.F., and Laurent, L.C. (2013). Matched miRNA and mRNA signatures from an hESC-based in vitro model of pancreatic differentiation reveal novel regulatory interactions. J. Cell Sci. *126*, 3848–3861.

Mendjan, S., Mascetti, V.L., Ortmann, D., Ortiz, M., Karjosukarso, D.W., Ng, Y., Moreau, T., and Pedersen, R.A. (2014). NANOG and CDX2 pattern distinct subtypes of human mesoderm during exit from pluripotency. Cell Stem Cell *15*, 310–325.

Moussaieff, A., Rouleau, M., Kitsberg, D., Cohen, M., Levy, G., Barasch, D., Nemirovski, A., Shen-Orr, S., Laevsky, I., Amit, M., et al. (2015). Glycolysis-mediated changes in acetyl-CoA and histone acetylation control the early differentiation of embryonic stem cells. Cell Metab *21*, 392–402.

Murry, C.E., and Keller, G. (2008). Differentiation of embryonic stem cells to clinically relevant populations: lessons from embryonic development. Cell *132*, 661–680.

Naujok, O., Diekmann, U., and Lenzen, S. (2014). The generation of definitive endoderm from human embryonic stem cells is initially independent from activin A but requires canonical Wnt-signaling. Stem Cell Rev. *10*, 480–493.

Rosa, A., and Brivanlou, A.H. (2011). A regulatory circuitry comprised of miR-302 and the transcription factors OCT4 and NR2F2 regulates human embryonic stem cell differentiation. EMBO J. *30*, 237–248.

Rosa, A., Papaioannou, M.D., Krzyspiak, J.E., and Brivanlou, A.H. (2014). miR-373 is regulated by TGFbeta signaling and promotes mesendoderm differentiation in human Embryonic Stem Cells. Dev. Biol. *391*, 81–88.

Rosa, A., Spagnoli, F.M., and Brivanlou, A.H. (2009). The miR-430/427/302 family controls mesendodermal fate specification via species-specific target selection. Dev. Cell *16*, 517–527.

Sakurai, H., Era, T., Jakt, L.M., Okada, M., Nakai, S., Nishikawa, S., and Nishikawa, S. (2006). In vitro modeling of paraxial and lateral mesoderm differentiation reveals early reversibility. Stem Cells *24*, 575–586.

Sayed, D., and Abdellatif, M. (2011). MicroRNAs in development and disease. Physiol. Rev. *91*, 827–887.

Stadler, B., Ivanovska, I., Mehta, K., Song, S., Nelson, A., Tan, Y., Mathieu, J., Darby, C., Blau, C.A., Ware, C., et al. (2010). Characterization of microRNAs involved in embryonic stem cell states. Stem Cells Dev. *19*, 935–950.

Tan, J.Y., Sriram, G., Rufaihah, A.J., Neoh, K.G., and Cao, T. (2013). Efficient derivation of lateral plate and paraxial mesoderm subtypes from human embryonic stem cells through GSKi-mediated differentiation. Stem Cells Dev. *22*, 1893–1906.

Wang, P., Rodriguez, R.T., Wang, J., Ghodasara, A., and Kim, S.K. (2011). Targeting SOX17 in human embryonic stem cells creates unique strategies for isolating and analyzing developing endoderm. Cell Stem Cell *8*, 335–346.

Wang, Y., Medvid, R., Melton, C., Jaenisch, R., and Blelloch, R. (2007). DGCR8 is essential for microRNA biogenesis and silencing of embryonic stem cell self-renewal. Nat. Genet. *39*, 380–385.

Xu, N., Papagiannakopoulos, T., Pan, G., Thomson, J.A., and Kosik, K.S. (2009). MicroRNA-145 regulates OCT4, SOX2, and KLF4 and represses pluripotency in human embryonic stem cells. Cell *137*, 647–658.

Yang, D., Lutter, D., Burtscher, I., Uetzmann, L., Theis, F.J., and Lickert, H. (2014). miR-335 promotes mesendodermal lineage segregation and shapes a transcription factor gradient in the endoderm. Development *141*, 514–525.

Supplemental Information

miRNome Profiling of Purified Endoderm and Mesoderm Differentiated from hESCs Reveals Functions of miR-483-3p and miR-1263 for Cell-Fate Decisions

Daichi Ishikawa, Ulf Diekmann, Jan Fiedler, Annette Just, Thomas Thum, Sigurd Lenzen, and Ortwin Naujok
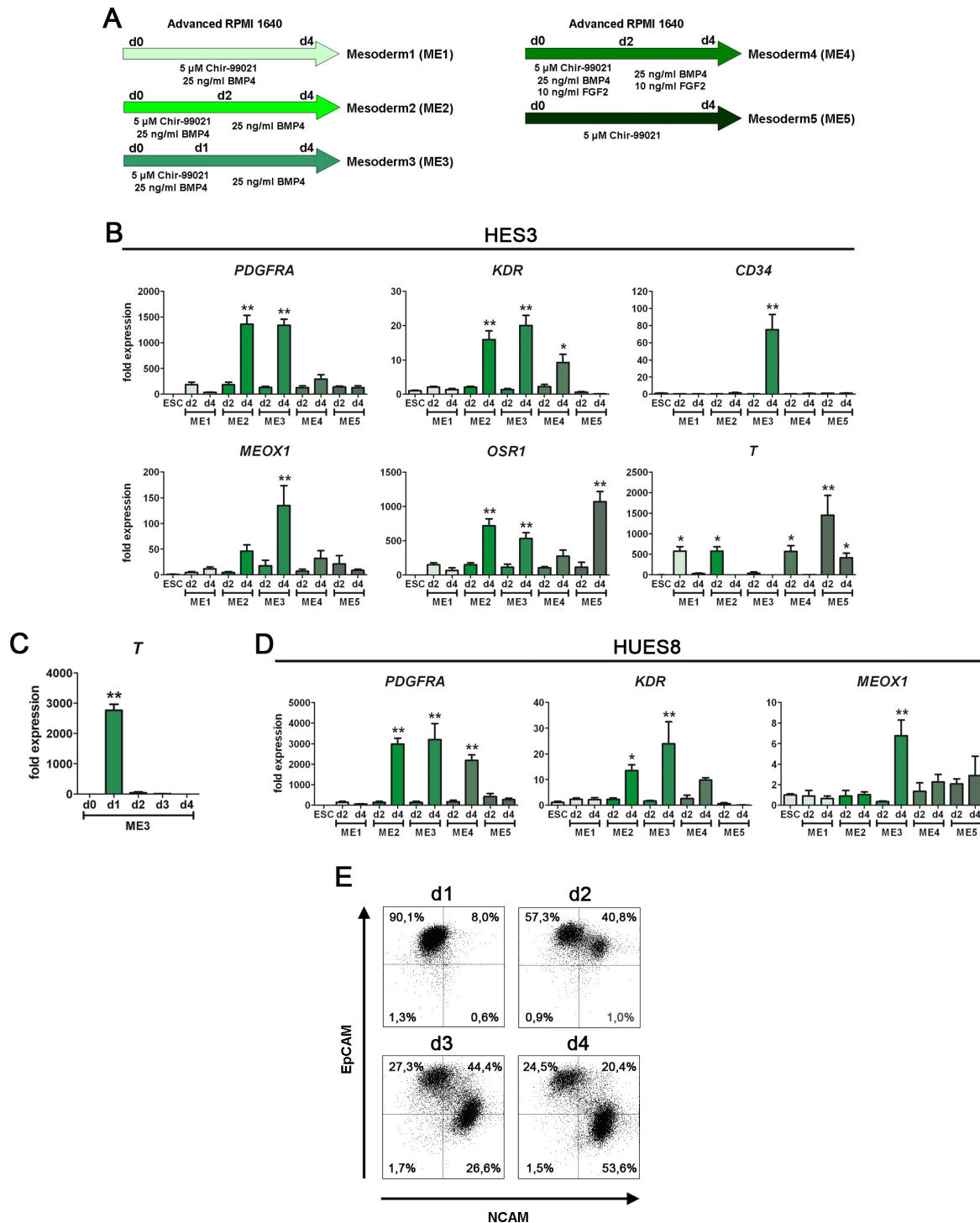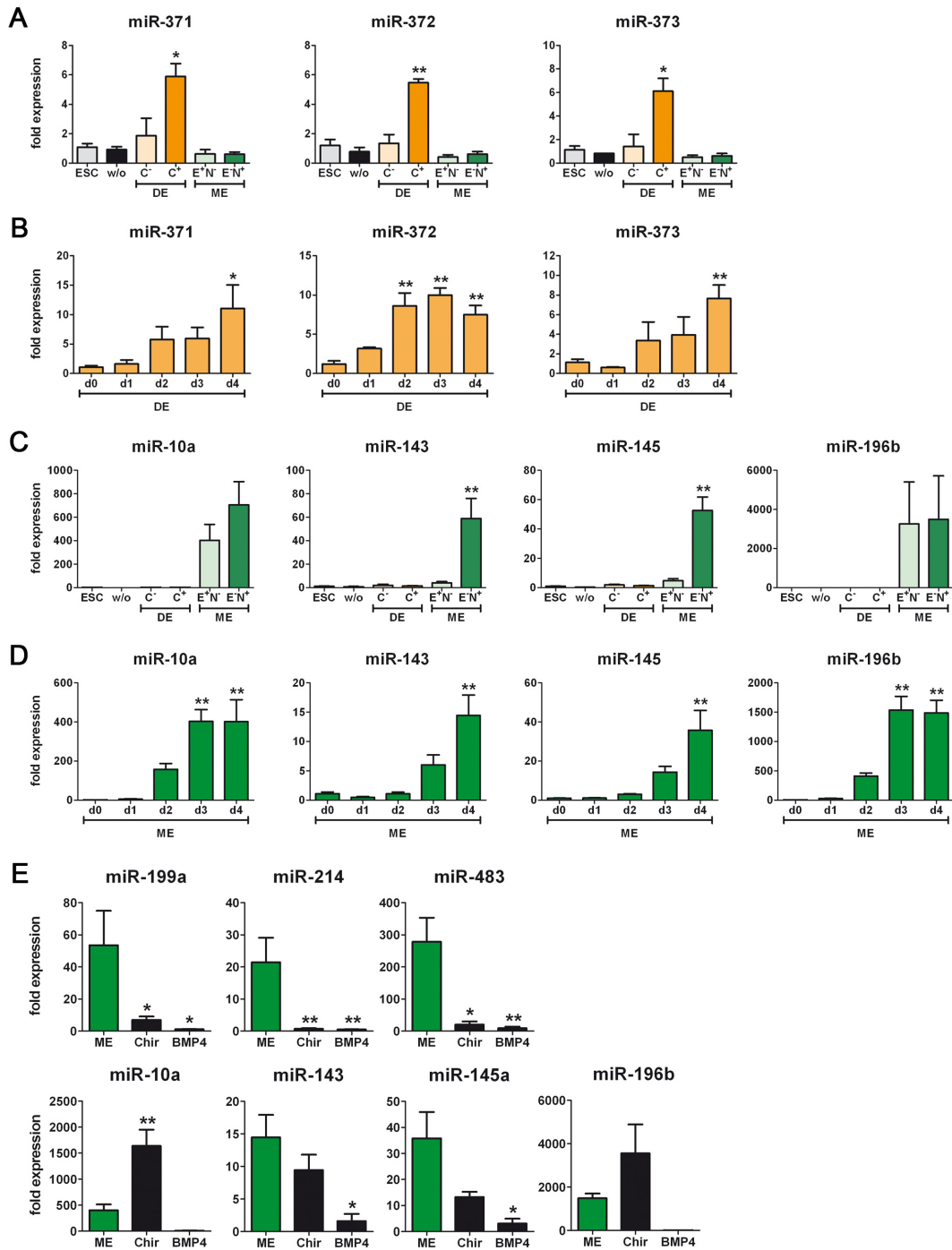
Supporting Information Figure S1. Protocols tested to induce mesodermal differentiation.

A) Depicted are the five different protocols tested for mesoderm (ME) differentiation and their abbreviations. **B**) Relative expression of the mesodermal marker genes (*PDGFRA*, *KDR*, *CD34*, *MEOX1*, *OSR1* and *T*) on day 2 and 4 of differentiation. **C**) Time course of the *T (Bry)* expression during differentiation with the ME3 protocol. **D**) Relative expression of the mesodermal marker genes (*PDGFRA*, *KDR*, *MEOX1*) on day 2 and 4 of differentiation with the indicated ME protocols using a second hESC line (HUES8). Gene expressions were normalized to three stably expressed housekeeping genes (*G6PD*, *TUB1A1*, *TBP*) and scaled to undifferentiated hESCs. Values are means ± SEM, n = 3-7. ANOVA plus *Bonferroni's post hoc test*, *p < 0.05, **p < 0.01 compared with hESCs. **E**) Representative flow cytometric dot plot diagrams of EpCAM/NCAM staining during differentiation with the ME3 protocol (HES3). Indicated numbers represent the percentages of cells in each quadrant.
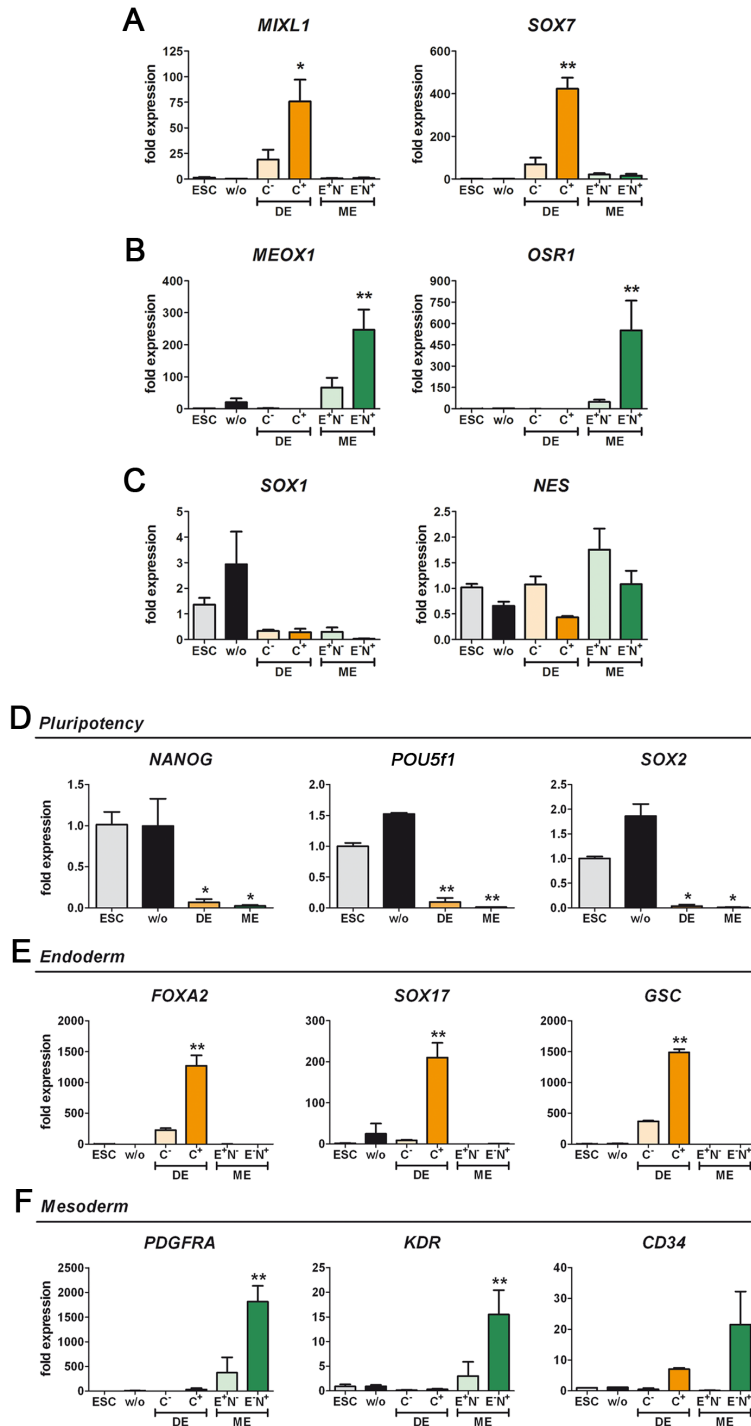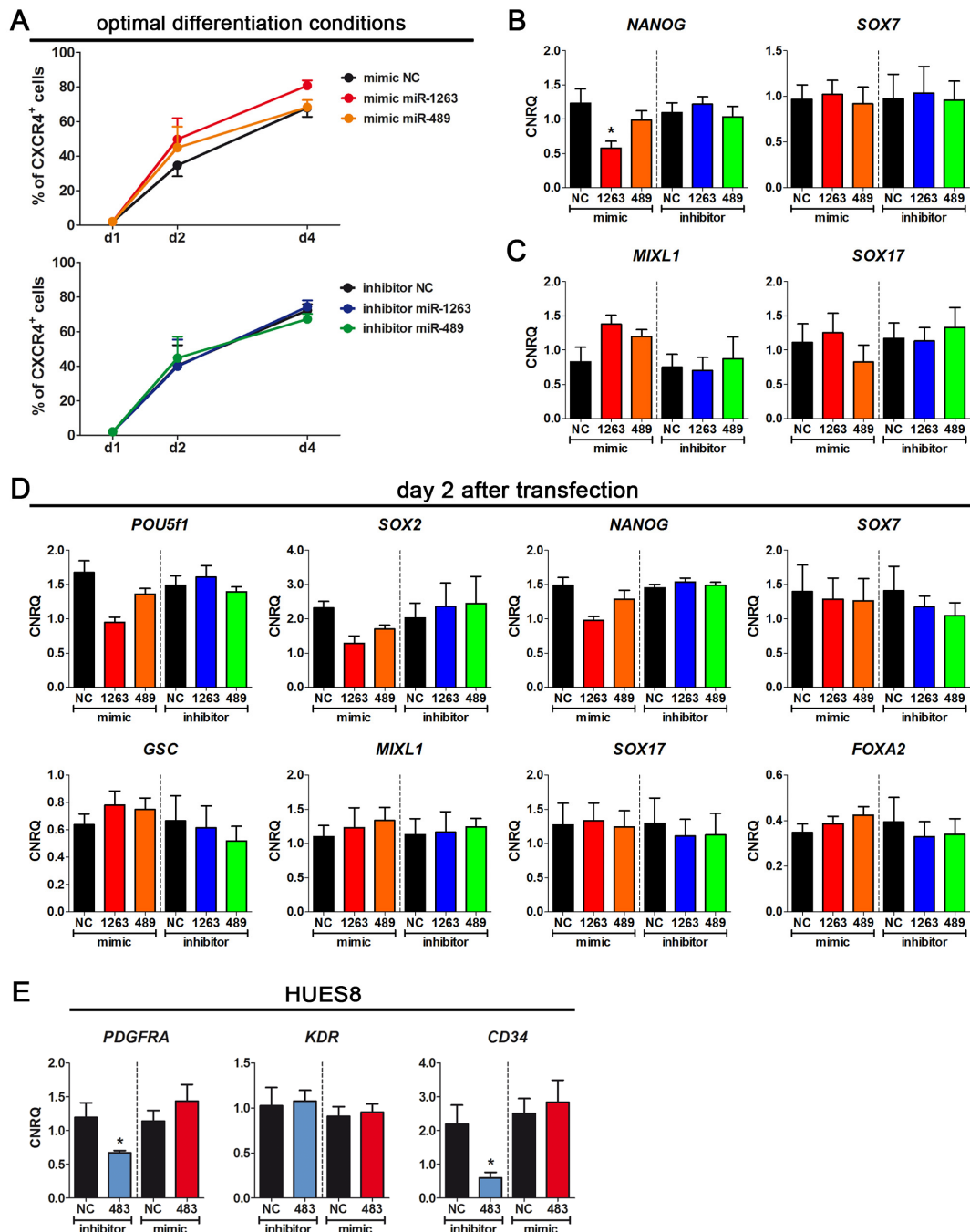
Supporting Information Figure S2. Gene expression analysis of additional lineage markers in different populations of HES3 and HUES8 cells.

Gene expression analysis in HES3 (**A-C**) and HUES8 cells (**D-F**). Depicted are early lineage markers (*MIXL1*, *SOX7*) (**A**), further mesoderm markers (*MEOX1*, *OSR1*) (**B**) and ectodermal markers (*SOX1*, *NES*) (**C**) in the specified populations (HES3). **D-F**) shows the relative expression of marker genes for pluripotency (*NANOG*, *OCT4*, *SOX2*) (**D**), endoderm (*FOXA2*, *SOX17*, *GSC*) (**E**) and mesoderm (*PDGFRA*, *KDR*, *CD34*) (**F**) in the different populations (HUES8). All gene expressions were normalized to three stably expressed housekeeping genes (*G6PD*, *TUB1A1*, *TBP*) and scaled to undifferentiated ESCs. Values represent means ± SEM, n = 3-7 (**A-C**), n = 3-5 (**D-F**). ANOVA plus Bonferroni's post hoc test, *p < 0.05, **p < 0.01 compared with hESCs in **D**, and compared with all other populations in **A-C** and **E/F**. Abbreviations: C⁻, CXCR4⁻ cells; C⁺, CXCR4⁺ cells; E⁺N⁻, EpCAM⁺/NCAM⁻ cells; E⁻N⁺, EpCAM⁻/low/NCAM⁺ cells; DE, definitive endoderm; ME, mesoderm; ESC, embryonic stem cells.

Supporting Information Figure S3. Validation of additional endoderm- or mesoderm-specific miRNAs.

A) Expression of additionally selected endoderm-specific miRNAs in the different populations. **B)** Time courses of their expressions during endoderm differentiation. **C)** Expressions of additional mesoderm-related miRNAs in the analyzed population. **D)** Expression kinetics of the additional mesoderm-specific miRNAs during ME differentiation. **E)** Comparison of mesoderm-specific miRNAs upon ME differentiation or upon exposure either to CHIR alone or to BMP4 alone. All miRNA expressions were normalized to the stably expressed housekeeping miRNAs RNU48, U6 snRNA and miR-425-5p and scaled to undifferentiated ESCs. Values are means ± SEM, n = 4-6. ANOVA plus *Bonferroni's post hoc test,* *p < 0.05, **p < 0.01 compared with all other populations in **A**/**C,** with undifferentiated cells on day 0 in **B**/**D** or with cells differentiated with ME protocol (**E**). Abbreviations: C⁻, CXCR4⁻ cells; C⁺, CXCR4⁺ cells; E⁺N⁻, EpCAM⁺/NCAM⁻ cells; E⁻N⁺, EpCAM⁻/low/NCAM⁺ cells; DE, definitive endoderm; ME, mesoderm; ESC, embryonic stem cells.
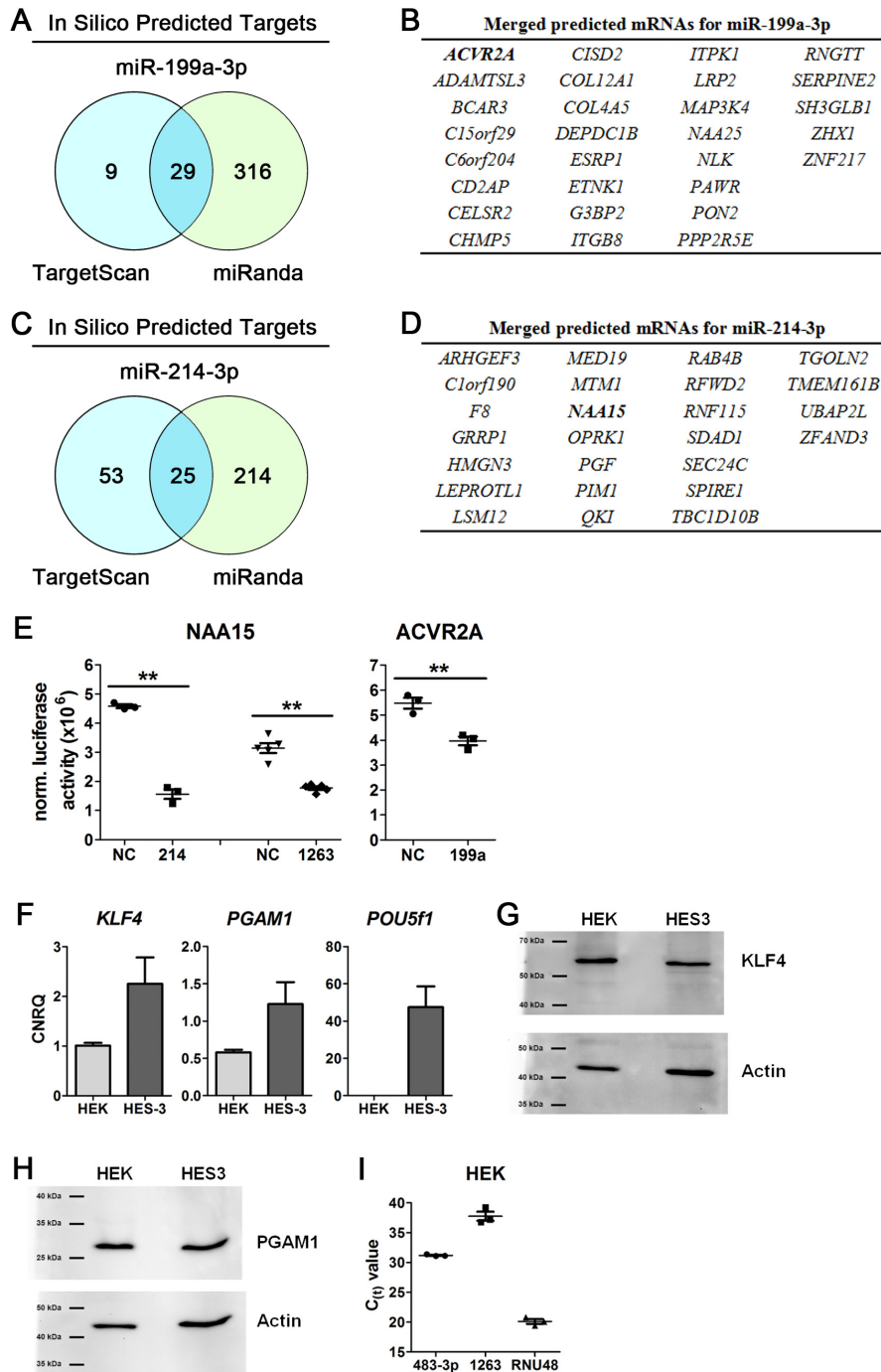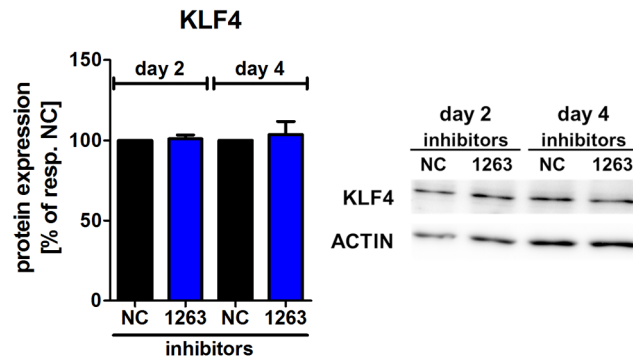
Supporting Information Figure S4. Gene and protein expression after transfection with endoderm- and mesoderm-specific miRNA mimics or inhibitors.

Two hESC lines were used in these experiments. In **A-D** are results shown using the HES3 line, while in **E** HUES8 cells were used. **A)** Time courses of the derivation of CXCR4$^+$ cells during optimal DE differentiation after transfection with mimics or inhibitors. Values are means ± SEM, n = 5-6. **B-C)** Normalized gene expression of markers for pluripotency (*NANOG*), extraembryonic endoderm (*SOX7*) (**B**) and primitive streak/DE (*MIXL1, SOX17*) (**C**) after four days of differentiation post transfection. Values are means ± SEM, n = 5-6. **D)** Normalized expression of pluripotency (*POU5F1, SOX2, NANOG*), extraembryonic endoderm (*SOX7*) and primitive streak/DE marker genes (*GSC, MIXL1, FOXA2, SOX17*) 2 days post transfection. Values are means ± SEM, n = 4-6. **E)** Normalized gene expression of mesodermal markers (*PDGFRA, KDR, CD34*) after transfection with miR-483-3p inhibitors/mimics using HUES8 cells. Values were scaled to undifferentiated ESCs and represent means ± SEM, n = 4-6. All expression values were normalized to the three stably expressed housekeeping genes. ANOVA plus *Bonferroni's post hoc test*, *p < 0.05, **p < 0.01 compared with cells transfected with miRNA inhibitor NC or mimic NC.

A In Silico Predicted Targets
miR-199a-3p

TargetScan: 9 | 29 | miRanda: 316

B Merged predicted mRNAs for miR-199a-3p

ACVR2A	CISD2	ITPK1	RNGTT
ADAMTSL3	COL12A1	LRP2	SERPINE2
BCAR3	COL4A5	MAP3K4	SH3GLB1
C15orf29	DEPDC1B	NAA25	ZHX1
C6orf204	ESRP1	NLK	ZNF217
CD2AP	ETNK1	PAWR	
CELSR2	G3BP2	PON2	
CHMP5	ITGB8	PPP2R5E	

C In Silico Predicted Targets
miR-214-3p

TargetScan: 53 | 25 | miRanda: 214

D Merged predicted mRNAs for miR-214-3p

ARHGEF3	MED19	RAB4B	TGOLN2
C1orf190	MTM1	RFWD2	TMEM161B
F8	*NAA15*	RNF115	UBAP2L
GRRP1	OPRK1	SDAD1	ZFAND3
HMGN3	PGF	SEC24C	
LEPROTL1	PIM1	SPIRE1	
LSM12	QKI	TBC1D10B	

Supporting Information Figure S5. In silico predicted target genes for miR-199a-3p and miR-214-3p plus the analysis of KLF4 and PGAM1 expression in HEK293 and HES3 cells.

Predicted targets of miR-199a-3p (**A-B**) and miR-214-3p (**C-D**) calculated by the TargetScan or miRanda algorithm. The merge of both data sets for the specific miRNA resulted in an overlap of 29 or 25 targets, respectively (**B** and **D**). **E)** Luciferase activity normalized to the β-galactosidase activity for the sub-cloned 3′-UTRs of *NAA15* and *ACVR2A* in HEK293 cells upon transfection with mimics and reporter plasmids. Values are means ± SEM, n = 4-6. *Student's t-test*, **p < 0.01. **F)** Gene expressions of *KLF4*, *PGAM1* and the pluripotency marker gene *POU5f1* in HEK293 (HEK) or HES3 cells. All values were normalized to the stably expressed housekeeping genes (*G6PD*, *TUB1A1*, *TBP*) and represent means ± SEM, n = 4. Western Blot detection of KLF4 (**G**) and PGAM1 (**H**) in these two cell lines. **I)** MiRNA expression as raw $C_{(t)}$-values of the ME-enriched mir-483-3p, the DE-enriched mir-1263 and an expressed control (RNU48) in HEK293 cells. The late $C_{(t)}$-values of ~32 and >35 for mir-483-3p and mir-1263, respectively, indicated a nearly absent expression in these cells. The depicted values are means ± SEM, n = 3.

Supporting Information Figure S6. MiRNA inhibitor for miR-1263 during endodermal differentiation of HES3 cells.

Normalized protein expression of KLF4 after transfection with the indicated miRNA mimics and differentiation under suboptimal DE condition. Additionally, a representative western blot of KLF4 for this experimental setup is depicted on the right. Values are means ± SEM, n = 4.

Supporting Information Table S1: Standard TaqMan qRT-PCR assays (Thermo Fisher Scientific) and used primer pairs for gene expression analysis.

Gene Symbol	Primer Sequence 5'-3'	Exon spanning	Accession #
CD34	TaqMan Assay: Hs02576480_m1		
FOXA2	Fw: gggagcggtgaagatgga Rev: tcatgttgctcacggaggagta	Yes	NM_153675.2
G6PD	Fw: aggccgtcaccaagaacattca Rev: cgatgatgcggttccagcctat	Yes	NM_000402
GSC	Fw: gaggagaaagtggaggtctggtt Rev: ctctgatgaggaccgcttctg	Yes	NM_173849.2
KDR	Fw: gacagtggtatggttcttgcc Rev: ctgcttcctcactggagtacac	Yes	NM_002253
MEOX1	TaqMan Assay: Hs00244943_m1		
MIXL1	Fw: ccgagtccaggatccaggta Rev: ctctgacgccgagacttgg	Yes	NM_031944.1
NANOG	Fw: ccgagggcagacatcatcc Rev: ccatccactgccacatcttct	Yes	NM_024864.2
NES	Fw: ctacagagccagatcgctcag Rev: ctagggaattgcagctccag	Yes	NM_006617
OSR1	Fw: ctacacctgtgacatctgccac Rev: cttcacctgtgagtgtagcgtc	Yes	NM_145260
PDGFRa	Fw: ccagagctatggggacttcc Rev: cttcactctccccaaagcatc	Yes	NM_006206
POU5F1	Fw: cttgctgcagaagtgggtggagg Rev: ctgcagtgtgggtttcgggca	Yes	NM_001173531.2
SOX2	Fw: agctacagcatgatgcagga Rev: ggtcatggagttgtactgca	Yes	NM_003106.3
SOX7 (v2)	Fw: gatgctgggaaagtcgtggaagg Rev: tgcgcggccggtacttgtag	Yes	NM_031439.3
SOX17	TaqMan Assay Hs00751752_s1		
SOX17_Sybr	Fw: gatgctgggcaagtcgtg Rev: ctgcatgtgctgcacgc	Yes	NM_022454.3
T	Fw: tgcttccctgagacccagtt Rev: gatcacttctttcctttgcatcaag	Yes	NM_003181.2
TBP	Fw: caacagcctgccaccttacgctc Rev: aggctgtggggtcagtccagtg	Yes	NM_003194
TUBA1A	Fw: ggcagtgtttgtagacttggaaccc Rev: tgtgataagttgctcagggtggaag	Yes	NM_006009

Supporting Information Table S2: Human TaqMan® miRNA qRT-PCR assays.

miRNA	Assay
hsa-mir-10a-5p	Assay-No.: 000387
hsa-miR-143-3p	Assay-No.: 000466
hsa-miR-145-5p	Assay-No.: 002278
hsa-miR-196b-5p	Assay-No.: 002215
hsa-miR-199a-3p	Assay-No.: 002304
hsa-miR-214-3p	Assay-No.: 002306
hsa-miR-371-3p	Assay-No.: 002124
hsa-miR-372-3p	Assay-No.: 000560
hsa-miR-373-3p	Assay-No.: 000561
hsa-mir-425-5p	Assay-No.: 001516
hsa-miR-483-3p	Assay-No.: 002339
hsa-mir-489	Assay-No.: 002358
hsa-mir-1243	Assay-No.: 002854
hsa-mir-1263	Assay-No.: 002784
RNU6B	Assay-No.: 001093
RNU48	Assay-No.: 001006
U6 snRNA	Assay-No.: 001973

Supplemental Experimental Procedures

Human ES cell culture

Cultivation of the hESC lines HUES8 and HES3 was performed under feeder-free conditions with minor modifications as described earlier (Diekmann et al., 2015; Diekmann and Naujok, 2016; Naujok et al., 2014). Briefly, hESCs were cultivated as colonies on tissue culture treated 6-well plates coated with hESC-qualified Matrigel (Corning, Amsterdam, Netherlands) in mTeSR™1 (Stemcell Technologies, Cologne, Germany) or StemMACS™ iPS-Brew XF (Miltenyi Biotech, Bergisch Gladbach, Germany) following the manufacturer's instructions. Passaging was performed every 5-7 days using an enzyme-free passaging solution (Nie et al., 2014) and the cells were re-seeded as small clusters in a ratio of 1:8-40 onto 6-well plates freshly coated with Matrigel in the respective cultivation medium.

Differentiation experiments

All differentiation experiments were initiated from dispersed single cells as described earlier (Diekmann et al., 2015). Briefly, hESC colonies were dissociated with enzyme-free Gentle Cell Dissociation Reagent (StemCell Technologies) or trypsin/EDTA (Thermo Fisher Scientific, Braunschweig, Germany), collected with Knockout-DMEM/F12 (Thermo Fisher Scientific), centrifuged for 3 min at 300x g and the cell pellet was resuspended in hESC cultivation medium containing 10 µM Y-27632 (Selleck Chemicals, Munich, Germany) prior to counting with the Cellometer Auto T4 (Nexcelom Bioscience, Massachusetts, USA). Subsequently, 95,000-100,000 cells/cm^2 (HUES8) or 65,000-75,000 cells/cm^2 (HES3) were seeded on dishes coated with Matrigel. Germ layer induction was initiated the next day after re-seeding. For induction of mesodermal (ME) and endodermal (DE) differentiation Advanced RPMI 1640 (Thermo Fisher Scientific) supplemented with 1% penicillin/streptomycin, 1% Glutamax (Thermo Fisher Scientific) and 0.2% FBS (PAA Laboratories, Germany, Cölbe) was used as base medium. Differentiation towards DE was performed by supplementation of the base medium with 50 ng/ml activin A (Peprotech, Hamburg, Germany) and 5 µM CHIR-99021 (Cayman Chemicals, Tallinn, Estonia) for 24 h followed by a 72 h treatment in the same medium without CHIR-99021. Suboptimal DE differentiation was performed accordingly to this protocol with the difference that the CHIR-99021 concentration was reduced to 2.5 µM (instead of 5 µM) for the first 24 h of DE differentiation. Induction of ME differentiation was performed in base medium supplemented with 25 ng/ml BMP4 (Peprotech) plus 5 µM CHIR-99021 for 24 h followed by cultivation in the same medium without CHIR-99021 for 72 h. Randomized differentiation was performed

applying solely the base medium. During differentiation the respective medium was changed every day.

Flow cytometry and cell sorting

For flow cytometry and fluorescence activated cell sorting (FACS) the cells were washed twice with PBS, dissociated with trypsin/EDTA, cetrifugated (700x g for 3min), resuspended in PBS plus 2% FCS and counted. For routine flow cytometry $1-2 \times 10^5$ cells were washed once and stained with primary conjugated antibodies in 100 µl PBS plus 2% FCS for 20-45 min at 4°C in the fridge. Unstained cells were used to set appropriate gates. Subsequently the cells were washed once or twice with 500 µl PBS plus 2% FCS and measured using a CyFlow ML flow cytometer (Partec, Münster, Germany). The subsequent analysis was performed with the FlowJo software (Ashland, OR, USA). For cell sorting $5-20 \times 10^6$ cells were stained with the respective primary conjugated antibodies as described above and FACS was performed at the central facility of Hannover Medical School using a XDP (Beckman-Coulter) cell sorter.

The following conjugated antibodies were used: anti-human CXCR4-APC (130-098-357, Miltenyi Biotec), anti-human CXCR4-PE (FC15004, Neuromics, Edina, MN, USA), anti-human CD49e-FITC (328008, BioLegend, London, UK), anti-human CD56/NCAM-BV510 (318340, BD Bioscience, Heidelberg, Germany), anti-human CD140a/PDGFRA-PE, anti-human CD326/EpCAM-PE (135905, 324206, BioLegend), anti-human CD34-APC, anti-human CD309/VEGFR2/KDR-VioBright FITC and CD309/VEGFR2/KDR-APC (130-090-954, 130-105-261, 130-093-604, Miltenyi Biotec).

Gene expression analysis

Total RNA was isolated using the peqGOLD RNAPure kit (Peqlab, Erlangen, Germany) and total RNA plus small RNAs using the miRNeasy Kit (Qiagen, Hilden, Germany) following the manufacturer´s instructions. Synthesis of cDNA was performed with random hexamer primers (Thermo Fisher Scientific) from 1,000-2,000 ng total RNA using the RevertAid™ H Minus M-MuLV Reverse Transcriptase (Thermo Fisher Scientific). For each qPCR reaction 5-10 ng of the initial total RNA was used from the cDNA samples. Every sample was amplified as triplicate using specific primer pairs or TaqMan® assays (Table S1) with the GoTaq® master mix (Promega, Mannheim, Germany) or TaqMan® Gene Expression Master Mix (Fisher Thermo Scientific) according to the manufacturer's instructions. All reactions were performed on a ViiA7 Real-Time PCR system (Thermo Fisher Scientific) and a melting curve analysis was performed to verify the correct amplification for SybrGreen-based PCR reactions. Data normalization was performed with qBasePlus (Biogazelle, Zwijnaarde,

Belgium) against the geometric mean of the three housekeeping genes *G6PD*, *TBP* and *TUBA1A*. Their stable expression was verified using the geNorm algorithm (M-values < 0.5) in qBasePlus.

MiRNA expression analysis

Reverse transcription was carried out with the TaqMan® MicroRNA Reverse Transcription kit (Thermo Fisher Scientific) using samples isolated with the miRNeasy Kit (Qiagen). For single miRNA assays 25 ng of total RNA with the small RNAs was reverse transcribed with sequence-specific primers (Table S2), whereas 500 ng were reverse transcribed for the miRNA array cards (v3.0) with the respective Megaplex™ RT primer pools (Thermo Fisher Scientific). For miRNA array cards each analyzed population represents a pooled sample from four independent experiments using equal RNA amounts to obtain the pooled sample. All TaqMan® miRNA assays and array cards were measured on the ViiA 7 Real-Time PCR system (Thermo Fisher Scientific). Raw-data of miRNA array cards were normalized applying the modified algorithm of the global mean normalization strategy (D'Haene et al., 2012) in qBasePlus. Data normalization of single miRNA assays was performed with qBasePlus against the stably expressed controls RNU48, U6 snRNA and hsa-mir-425-5p (M-values < 0.5, geNorm algorithm).

MiRNA transfection experiments

For transfection of miRNA inhibitors or mimics (Thermo Fisher Scientific) Lipofectamine® 2000 transfection reagent (Thermo Fisher Scientific) was used as instructed by the manufacturer´s protocol. Briefly, 3 µl of Lipofectamine® 2000 was diluted in 100 µl of Opti-MEM medium (Thermo Fisher Scientific) and mixed with 30 pmol of the respective miRNA inhibitor or mimic. After incubation for 5 min at room temperature the miRNA-lipid complex was added dropwise to the culture medium of the cells. The medium was changed the next day (18-24 h). During DE differentiation the miRNA inhibitors or mimics were transfected on day 0 by changing to the first DE differentiation medium and subsequent transfection with the next 10-30 min. During ME differentiation transfection was performed on day 2 of differentiation. Therefore, one to three hours prior transfection differentiated cells were dissociated with trypsin/EDTA, counted and 7.5×10^4 cells/cm^2 seeded onto 12-well plates coated with Matrigel in mesoderm differentiation medium containing 10 µM Y-27632. This step was performed to reduce the high confluency on day 2 and thereby reaching acceptable transfection efficiencies. For each experiment the transfection efficiency was examined by transfecting a FAM-conjugated negative control that was analyzed one day post transfection

by flow cytometry. For further analysis only experiments with a chosen cut-off of 60% positive cells 24 hrs post transfection were used.

SiRNA transfection experiments

Transfection of siRNAs (Thermo Fisher Scientific) was performed with Lipofectamine® 2000 transfection reagent as instructed by the manufacturer. The siRNA transfection procedure was similar performed as described above for the miRNA mimic/inhibitor transfections. Briefly, transfection at day 0 of DE differentiation were performed with 5 µl Lipofectamine® 2000 and 5 µl siRNA (10 pmol) per 12-well diluted in 100 µl Opti-MEM medium. Subsequently, the complexed siRNA was added dropwise to the cells, which already had received the media for DE differentiation. For the transfection during ME differentiation the cells were re-seeded at day 2 as described above and transfected with 3 µl Lipofectamine® 2000 and 3 µl siRNA (10 pmol) per 12-well. A FAM-conjugated negative control was used to determine the transfection efficiency 24 h post transfection by flow cytometry. Also a second unlabeled negative control was used as an additional control to exclude an effect of the FAM-labeling of the siRNA negative control.

Luciferase Reporter Assay

Partial 3'UTRs of genes that harbor at least one potential binding site for the respective miRNA were individually cloned into the SpeI/HindIII cloning site of the pMIR-REPORT vector (Thermo Fisher Scientific) behind the sequence that encodes the luciferase gene. HEK293 cells seeded in 48-well-plates were co-transfected with 20 ng of the particular luciferase reporter construct, 20 ng β-galactosidase control plasmid (Promega, Mannheim, Germany) and 30 nM of either control miRNA or the respective miRNA mimic using Lipofectamine® 2000. The transfected cells were incubated 24 h prior to detection of the luciferase and the β-galactosidase activity by applying the different substrates (Promega). Data normalization was performed with the measured β-galactosidase activity of the respective sample.

Western Blot analysis

The cells were dissociated with trypsin/EDTA, centrifuged for 3 min at 700x g and resuspended in RIPA buffer (Thermo Fisher Scientific). These whole cell extracts were additionally sonified with 6 pulses of 60% amplitude and 0.8 cycle using a Labsonic M sonificator (Sartorius, Göttingen, Germany). Subsequently, complete protease inhibitor mixture (Roche Diagnostics, Manheim, Germany) was added to the extracts. The protein content was determined by BCA assay (Thermo Fisher Scientific) and 10-20 µg of total

protein was separated by a 12.5% SDS-PAGE followed by transferring the proteins to a PVDF (polyvinylidene fluoride) membrane via electro-blotting. Nonspecific binding was blocked for 1 h at room temperature with 2% or 5% nonfat dry milk in PBS plus 0.1% Tween 20. Thereafter, the membranes were incubated with primary antibodies overnight at 4 °C. After three washing steps (PBS, 0.1% Tween 20) they were incubated with peroxidase-labeled secondary antibodies (711-035-152, diluted 1:40,000 and 115-035-166, diluted 1:10,000, Dianova, Hamburg, Germany) at room temperature for 1 h. The bands were visualized by chemiluminescence using the ECL select or the ECL detection kit (GE Healthcare Europe, Freiburg, Germany) with an automated chemiluminescence imager (INTAS Science imaging, Göttingen, Germany). Densitometic analysis was performed with the Image Studio Lite software (LI-COR, Bad Homburg, Germany).

The following specific antibodies were used: anti-KLF4 (ab72543, diluted 1:1000, Abcam, Cambridge, UK), anti-PGAM1 (#12098, diluted 1:1000, Cell Signaling Technology, Leiden, Netherlands) and anti-ß-ACTIN (sc-47778, diluted 1:1000, Santa Cruz Biotechnology, Dallas, USA).

Statistics

Unless stated otherwise all data values represent means ± SEM. In each figure legend the respective number of independent experiments is stated (n). Statistical analyses were performed using the GraphPad Prism software (Graphpad, San Diego, CA, USA) using *Student's t-test* or ANOVA followed by *Bonferroni's* or *Dunnett's post hoc* test for multiple comparisons.

Supplemental References

D'Haene, B., Mestdagh, P., Hellemans, J. & Vandesompele, J. 2012. miRNA expression profiling: from reference genes to global mean normalization. *Methods Mol Biol,* 822**,** 261-72.

Diekmann, U., Lenzen, S. & Naujok, O. 2015. A reliable and efficient protocol for human pluripotent stem cell differentiation into the definitive endoderm based on dispersed single cells. *Stem Cells Dev,* 24**,** 190-204.

Diekmann, U. & Naujok, O. 2016. Generation and Purification of Definitive Endoderm Cells Generated from Pluripotent Stem Cells. *Methods Mol Biol,* 1341**,** 157-72.

Naujok, O., Diekmann, U. & Lenzen, S. 2014. The generation of definitive endoderm from human embryonic stem cells is initially independent from activin A but requires canonical Wnt-signaling. *Stem Cell Rev,* 10**,** 480-93.

Nie, Y., Walsh, P., Clarke, D. L., Rowley, J. A. & Fellner, T. 2014. Scalable passaging of adherent human pluripotent stem cells. *PLoS One,* 9**,** e88012.